Title

Measured influence of overhead HVAC on exposure to airborne contaminants from simulated speaking in a meeting and a classroom

Journal

Indoor Air, 32(1)

ISSN

0905-6947

Authors

Singer, Brett C

Zhao, Haoran

Preble, Chelsea V

et al.

Publication Date

2022

DOI

10.1111/ina.12917

Peer reviewed

Measured Influence of Overhead HVAC on Exposure to Airborne Contaminants from Simulated Speaking in a Meeting and a Classroom

Brett C. Singer[1]*, Haoran Zhao[1], Chelsea V. Preble[1,2], William W. Delp[1], Jovan Pantelic[1,3], Michael D. Sohn[1], Thomas W. Kirchstetter[1,2]

[1]Indoor Environment Group, Energy Analysis and Environmental Impacts Division, Building Technologies and Urban Systems Division, Energy Technologies Area, Lawrence Berkeley National Laboratory, Berkeley, CA, USA

[2]Department of Civil & Environmental Engineering, University of California, Berkeley, CA, USA

[3]Center for the Built Environment, University of California, Berkeley, CA, USA

Abstract

Tracer gas experiments were conducted in a 158 m^3 room with overhead supply diffusers to study dispersion of contaminants from simulated speaking in physically-distanced meeting and classroom configurations. The room was contained within a 237 m^3 cell with open plenum return to the HVAC system. Heated manikins at desks and a researcher operating the tracer release apparatus presented 8–9 thermal plumes. Experiments were conducted under conditions of no forced air and neutral, cooled, or heated air supplied at 980–1100 cmh, and with/out 20% outdoor air. CO_2 was released at the head of one manikin in each experiment to simulate small (<5 μm diameter) respiratory aerosols. The metric of Exposure Relative to perfectly-Mixed (ERM) is introduced to quantify impacts, based on measurements at manikin heads and at three heights in the center and corners of the room. Chilled or neutral supply air provided good mixing with ERMs close to one. Thermal stratification during heating produced higher ERMs at most manikins: 25% were ≥2.5 and the highest were >5× perfectly mixed conditions. Operation of two within-zone air cleaners together moving ≥400 cmh vertically in the room provided enough mixing to mitigate elevated exposure variations.

Keywords

Airborne infectious disease; COVID-19; Expired bioeffluents; Respiratory aerosols; Ventilation effectiveness; FLEXLAB

Practical Implications

- Overhead HVAC systems, which are common in schools and office buildings, can create thermally stratified conditions during heating.
- Stratification interferes with dilution and reduces the effectiveness of ventilation to remove expelled respiratory aerosols that can carry infectious agents.
- Ceiling diffusers can achieve good mixing for effective dilution and ventilation of bioeffluents when supplying cooled or thermally neutral air.
- Fans, including portable air filters, can break up stratification and improve ventilation performance during the heating season.

Introduction

It is well established that effective ventilation, filtration, and airflow management can reduce the risk of airborne infectious disease transmission in healthcare settings. The pandemic caused by the SAR-CoV-2 virus has raised awareness that the same types of engineering controls can be applied to reduce airborne transmission risk in all buildings[1,2].

The SARS-CoV-2 virus is one of several infectious microorganisms that may be transmitted via respiratory aerosols that are emitted during coughing, sneezing, vocalization and breathing, even by asymptomatic infected persons[3–5]. Despite uncertainty about the relative importance of droplets and aerosols of various sizes as mediators of transmission, there is direct evidence of viruses in respiratory aerosols smaller than 5 μm expelled by infected persons[6–9] and evidence that those respiratory aerosols can transfer infectious quanta of virus between people occupying the same enclosed spaces[10,11].

Since the gravitational settling times of aerosols <5 μm in diameter are longer than 10 min[12–15], they can remain airborne to mix throughout a building. Environmental sampling in healthcare settings with COVID-19 patients has confirmed the presence of SARS-CoV-2 virus in airborne aerosols under 4 μm[16–21], on ceiling diffusers which are likely to be reached only by smaller aerosols[18,19], and in an HVAC system[22]. Experiments have also demonstrated that the SARS-CoV-2 virus can remain viable in aerosol form for hours[23,24].

Some carefully studied outbreaks are most easily explained by airborne transmission via aerosols remaining in the air for minutes to hours[25–30]. These studies are supported by simulations finding substantial transmission risk from small aerosols when an infectious individual is in an enclosed space with others, with risk related to the size of the room, ventilation, filtration, and duration of exposure[10,31]. Modeling of close interactions indicates that small aerosols may comprise a significant fraction of virus transfer even during close contact events which include larger aerosols and ballistic droplets.[32]

Recognizing the potential for airborne transmission—especially indoors—public health agencies and experts recommend a layered risk management approach that includes face coverings for source reduction, maintaining distance to reduce the risk of direct transfer, engineering controls to reduce virus concentrations and also connections between occupants, and respirators (which also serve as face coverings) as personal protective equipment. Engineering controls that are known to be effective at reducing pathogen levels in indoor air include ventilation, dilution with air supply[33], filtration in the HVAC system,[34,35] in-zone filtration[36], and in-zone ultraviolet germicidal irradiation[37–39].

There is broad agreement that bulk airflow and mixing patterns can influence transfer risks for airborne infectious agents[40–42]. In the indoor environment, drivers of air movement include air supply systems, open windows[43], heat sources, human activities[44], and door use[44,45]. The impacts of various air supply configurations on potential airborne transfer have been studied extensively for hospitals[46,47] and offices[33,41,48–52], using cooled or thermally neutral supply air (i.e., same temperature as the room). Many studies have shown that an increase in air supply leads to reduced exposure and risk of cross-infection[53], while some have reported that increasing the air supplied to a space can lead to increased exposure and risk of cross-infection [46,49]. These latter studies demonstrated that the airflow patterns induced by some air distribution system designs can cause closer connections between occupants as airflow is increased. Studies using aerosol release as surrogates under thermally neutral supply air conditions have concluded that bulk

room airflow patterns drive dispersion of potentially infectious aerosols more than turbulent dispersion of the expired respiratory emissions [54–56]. Several studies have reported on the negative impacts of thermal stratification with overhead heating, using metrics of air change efficiency/effectiveness and contaminant removal effectiveness in room-scale chambers with 1–2 thermal manikins [57,58] or chambers without internal thermal sources.[59,60]

As indicated in the brief literature summary, there are relatively few studies of the effect of imperfect mixing on human-expelled contaminant dispersion in fully-sized rooms with operational occupancy (i.e., more than 1–2 simulated test subjects), and also few which focused on the potential impacts of stratification when heating with overhead diffusers.

To address these gaps, we conducted experiments to investigate the impacts of ceiling HVAC supply air thermal conditioning on dispersion and mixing of a gaseous surrogate for small respiratory aerosols, focusing on physically-distanced meeting and classroom scenarios. Under low air velocities that are typical for these room scenarios (<1 m s^{-1}) and characteristic length scales that represent bulk air flow (~0.5 m) and much smaller scales relevant to flows around objects such as warm bodies, particles <5 µm generally follow fluid streamlines (Stokes number << 1). The characteristic time for these particles to settle from a height of 1.5 m in quiescent air ranges from 482 hours for 0.1 µm aerosols to 8 minutes for 10 µm particles. Previous studies have assumed tracer gases act as a proxy for the dispersion behavior of small respiratory aerosols [61–63], while others have simulated or experimentally shown that tracer gases adequately represent the movement of particles that are no larger than 5 µm in diameter [64–69]. With a series of experiments under operational occupancy conditions and various supply air scenarios, this manuscript addresses an important aspect of engineering controls and evaluates how overhead heating can interrupt mixing within a room, thereby reducing the benefits of ventilation and leading to elevated exposures in the breathing zone.

Methods

Overview

Experiments were conducted to investigate dispersion and mixing of a contaminant emitted from a single simulated speaker in a room with tables arranged for a physically-distanced meeting or classroom. We focused on speaking rather than coughing or sneezing as the dramatic emission events are less common and may be expected to result in the symptomatic attendee being asked to leave the room. The meeting room was operated without mechanical airflow or with neutral, cooled, or heated supply air. Outdoor air was provided in a subset of experiments. Human thermal plumes were approximated with heated manikins. Emissions of respiratory aerosols <5 µm in diameter were simulated by release of carbon dioxide (CO_2) tracer gas. The study included exploratory experiments to assess the mixing benefits of operating portable air cleaners to counter stratification and placing a standing barrier in front of the simulated teacher in the classroom. Dynamics of 8–10 µm aerosols released with CO_2 in selected experiments will be reported in a subsequent paper. The main outcomes presented here are the observed spatial variations of CO_2 tracer and resulting variations in exposure concentrations within the vertical middle of the room (~0.9–1.8 m height), where occupants would both emit and inhale respiratory aerosols, i.e., the breathing zone. The main outcomes are the integrated exposures at the heads of thermal manikins representing meeting participants or students, and the ratios of those integrated exposures to those that would occur with ideal mixing under the same bulk room conditions.

Physical Chamber Configurations

Experimental Room and HVAC

Experiments were conducted in Cell 3A of the FLEXLAB facility at Lawrence Berkeley National Lab (https://flexlab.lbl.gov). The cell is 6.10 m east–west by 9.34 m north–south (N-S). The full height from the concrete slab to the foam-covered bottom of the roof is 4.04 m at the north end sloping up to 4.21 m at the south end, creating an estimated volume of 237 m^3. A panelized hanging ceiling at 2.74 m sets the boundary of a 158 m^3 room in the bottom portion of the cell. The above-ceiling plenum serves as the return path for the air handling unit (AHU) and houses the four supply diffusers. A schematic of the room is provided in Figure 1.

The south wall has aluminum-framed windows (with thermal break) in five horizontal sections that start at 0.91 m and extend to the top of the room at 2.74 m. The glazing has a solar heat gain coefficient (SHGC) of 0.25 and U-value of 0.60, consistent with the ASHRAE 90.1-2010 standard. For the simulated meeting room experiments, the windows were covered on the outside with 5 cm thick, foil-faced polyisocyanurate panels that were cut to overlap with each window frame and secured with metal tape along all edges (Figure S1). This was done to limit the heat flux at the windows. Foam panels were removed from the second and fourth window sections (each 1.22 m wide) for the classroom experiments (Figure S2 to Figure S4), as classrooms typically have windows. The walls that separate Cell 3A from adjacent cells to the east and west extend from the concrete slab to the roof. The sections of south wall below and above the windows were built to the standards of ASHRAE 90.1-2010 with 15 cm of R-13 batt insulation and steel studs behind nominal 1.3 cm plywood and 1.9 cm R-3.5 rigid insulation to provide a thermal break and moisture barrier. The north wall is sectioned to include a closet that houses the HVAC system, which is accessed from the interior wall via a weather-stripped door.

Ventilation and thermal conditioning for the cell are provided by a fully-controllable forced air system. The volumetric airflow was controlled via the variable frequency drive of the AHU. Outdoor air (OA) was controlled by setting outdoor, return, and exhaust air damper positions and monitoring flow rates measured separately at the intake, return, and exhaust. Supply air temperature was controlled by manipulating hot and chilled water loops while the supply temperature was monitored in real time.

Air was supplied to the room via two or four ceiling mounted perforated plate diffusers (Titus-PPS), each with a 30-cm diameter neck and 60-cm square presentation, with locations shown in Figure 1. Air is removed from the room and directed to the AHU return and/or exhausted from the cell via the open plenum above the false ceiling. The room was connected to the plenum by removing a single 60-cm square ceiling tile. The most commonly used opening to the return was at the northeast (NE) corner of the room, very close to the AHU. In some experiments, the return was placed at the southwest (SW) corner or just south of the center (CTR) of the room, at locations shown in Figure 1. In some experiments the NE and SW supply air diffusers were covered to increase exit air velocities at the other diffusers.

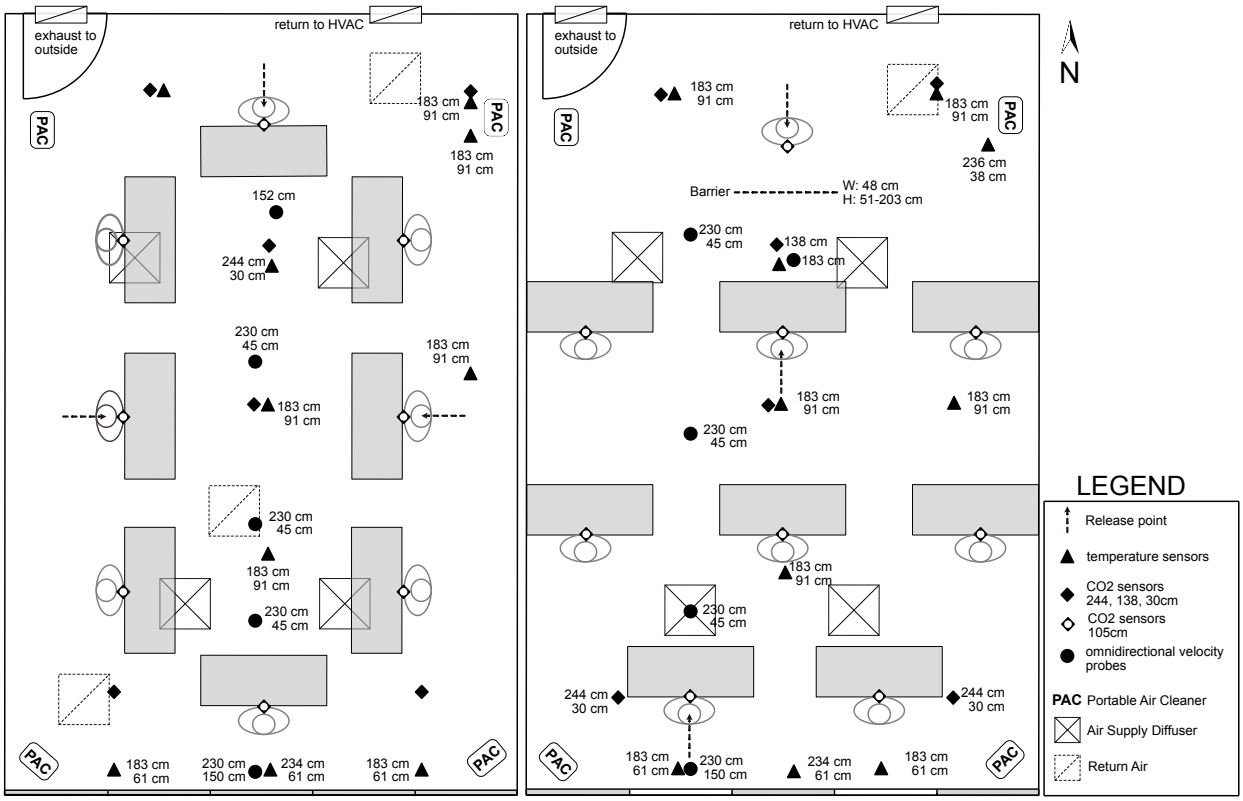

Figure 1: Manikin and sensor locations in (a) Meeting and (b) Classroom configurations. Distances next to each sensor type indicate sensor deployment heights. CO_2 and temperature sensors were at the locations shown through most Meeting and all Classroom experiments. Anemometers were deployed in various arrangements in the Meeting room. Hatched lines used for features that varied in location across experiments. Each experiment featured only one opening to return plenum, as shown in Table 1.

Four portable air cleaners (PACs) (Winix Model 5300-2) were placed in the corners of the cell and operated before experiments to mix the air and reduce particle levels. They were also operated during several experiments with heating to assess their potential to break stratification and reduce variations in exposure concentrations. On the highest setting, each PAC provides a rated clean airflow of 408 cmh using HEPA filtration and including a thin active carbon prefilter. The four PACs together provided an airflow of at least 1632 cmh. PACs of the size used in this study are widely available for a cost (excluding taxes) under US$200/unit.

A free-standing barrier deployed in one meeting and six classroom experiments was 130 cm wide and had thick plastic sheeting from 51 to 203 cm above the floor. The barrier is shown in Figure S5 and its location noted in Figure 1.

Occupancy Configurations

A physically-distanced meeting was arranged as shown in Figure 1a, which is drawn to scale. A photograph of the room with desks and manikins is shown in Figure S6. Eight tables were arranged to provide 2.13 m between the heads of adjacent manikins. Tables were 1.52 m long, 0.60 m wide, and 0.74 m tall. All windows were covered with foam insulation for all meeting experiments and various combinations of supply diffusers (2 vs. 4), return plenum opening (SW, CTR, NE), and airflow conditions were implemented (See Table 1).

A physically-distanced classroom was set up as shown in Figure 1b, with nine occupant positions including eight simulated students and one teacher. A photograph of the room with desks and manikins is shown in Figure S5. The same eight tables from the meeting were arranged in three rows to achieve a distance of 2.29 m between the heads of adjacent "students." The front face of the "teacher" was 2.94 m from the "student" in the center of the front row (R1C), when both positions were occupied by manikins. For this configuration, foam panels were removed from two non-adjacent, non-edge window panels. Metal blinds installed on the inside of the windows were swiveled to reflect incoming direct sunlight but allow diffuse natural light into the chamber, as shown in Figure S3.

Simulated Occupant Thermal Plumes & Other Heat Sources

Eight manikins with heating tape wrapped around their legs, torso, arms, and head simulated human thermal plumes. Six manikins dispersed 76–77 W and the other two were 89 and 127 W. The manikins wore clothing with estimated thermal properties of approximately 0.6 clo (socks, trousers, long sleeve shirt/blouse). For some experiments, a researcher had to be present in the chamber to operate an aerosol source. When present, the researcher sat just behind and to one side of an aerosol generator that was used as a tracer release mechanism, as described below, and did not move from the chair during the experiment. Given the researcher's activity level, her heat output during experiments is assumed to be within the range of the manikins. The experiments with the researcher present are indicated in Table 1. Other heat sources included the CO_2 meters and pumps, particle counters, anemometers, laptops for logging data, and the heating device for tracer release, together added a total of ~250–300 W during the experiments (see SI).

During the meeting room experiments, which mostly occurred from mid-afternoon through early evening, there was some heat flux into the room via the south wall. Measured values of the direct solar heat flux on the exterior of the south wall are provided in Figure S7. For the classroom experiments, there was solar gain through the two uninsulated window sections. The amount of radiative heat flux was estimated as the product of the direct irradiance on the south wall and window, the SHGC, and the exposed window area of 4.5 m^2. These heat flux values varied from about 170 W for experiments conducted in the morning to 580 W for late afternoon experiments.

Tracer Releases

Mixtures of CO_2, air, and sometimes particles were released from variations of three assemblies, as described and shown in the SI. The assemblies were changed to incorporate particle releases of different sizes, monitor those particle release rates, and in most cases to achieve releases at close to body temperature. The release tubes had cross-sectional internal areas of 0.71, 0.97, and 1.8 cm^2, used respectively in 4, 16, and 28 experiments. Mouth opening area varies through the course of a vocalization and an estimated average opening of 1.8 cm^2 was suggested by Gupta et al.[70] Releases were heated in 33 experiments to temperatures of 33–42 ºC, with most (n=30) in the range of 35–40 ºC . Gaseous tracer releases in most experiments were 5.1 LPM of CO_2 with 10 LPM air; exceptions were three experiments that released only 5.7 LPM air with the 5.1 LPM CO_2 release and six experiments that released 2.55 LPM CO_2, one with 8 LPM air and five with 10 LPM air. These total volumetric flow rates are slightly higher than the mean estimated rate reported for reading a passage, but lower than those for counting or saying the alphabet (ibid). The CO_2 release rates are roughly 20 times those of human expiration.[71,72]

Each experiment featured a single release from one location. There were three release locations in the meeting configuration, with tracer releases adjacent to the heads of the manikins in the

west (n=19), north (n=13) or east (n=5) positions. There were 30 releases at the height of a standing adult (most commonly at 152 cm) and 19 at a height of 109 cm to represent seated speakers. In the classroom, there were also three release locations, with four releases from the Teacher position at standing height, four from the seated middle of the front row (R1C), and three from the center-west of the back row (R3C) at seated height.

Summary of Experimental Conditions

Twenty-nine experiments were conducted without outdoor air ventilation to focus on the effects of supply air and temperature on mixing and exposures in the meeting room; conditions for these are summarized in Table 1. These included nine experiments with no forced air (no AHU), three with cooling, five with unconditioned airflow, and twelve with heated airflow, including two with PACs operating. When the AHU was off, air movement was induced by the thermal plumes of the manikins and electronics in the room and presumably also by heat transfer at the south facing wall. Two supply diffusers were covered in twelve of the 20 experiments with AHU operating without ventilation (i.e., recirculating air only), including the two experiments with PACs. When all four diffusers were used, the neck velocity was approximately 1 m s^{-1}, and when only two were used the neck velocity was 2 m s^{-1}. Air speeds measured at various points 2.5 cm below the diffuser peaked at roughly 1.5 m s^{-1} when only two diffusers were used and roughly half those values when all four diffusers were used. The room-to-plenum opening was in the southwest corner in five experiments and just south of the center in three (see Figure 1); it was in the northeast corner in the other 12 of 20 mixing-only experiments.

Outdoor air was provided at roughly 20% of the supply airflow of 1000–1070 cmh (4.2–4.5 ach) in eight experiments in the meeting configuration and 11 classroom experiments, all with four supply diffusers and the return opening in the NE position. The meeting experiments were split between neutral and heated supply temperatures and classroom experiments were roughly split between cooling and heating.

Two of the portable air cleaners, positioned in the corners of the room, were operated on the highest setting during two releases with heat and no OA ventilation. One PAC was operated on its highest setting during one experiment with heating and 20% OA.

The standing barrier was placed between the Teacher and the R1C student position for roughly half of the classroom experiments, in a matrix that varied supply temperature, release position, and barrier presence (Table 1).

Measurements

HVAC Airflows and Temperatures

Supply and outdoor air flow rates were measured using Ebtron Advantage II Gold Series, GP1 type A probes with GTX116 transmitters that were calibrated in situ approximately 2 years prior to these experiments. Supply and return air temperatures (SAT, RAT) were measured with BAPI 10K-2 thermistor probes that were inserted into the ducts. These probes were last calibrated 5-years ago, such that an expected 0.02 ºC y^{-1} drift in their listed accuracy of ±0.1 ºC should limit any error to <0.2 ºC.

Carbon Dioxide

Carbon dioxide concentrations were measured using fast response non-dispersive infrared (NDIR) sensors (CO2Meter, K30 model SE-0117), which were connected to Raspberry Pi

computers via USB developer kits that logged data at 1-second intervals. Each K30 sensor was connected to an external pump drawing air at a flow rate of ~0.5 LPM to enable fast response. CO_2 data were obtained from a total of 22–26 measurement points per experiment. Fifteen CO_2 sensors were deployed at heights of 30, 137, and 243 cm on five poles located in each corner and in the center of the room (Figure 1). A CO_2 sensor was placed at the neck of each manikin. In some experiments, up to three additional CO_2 sensors were placed at other locations of interest. The CO_2 sensors were calibrated to each other and to a PP Systems Model SBA-5 NDIR CO_2 analyzer, which sampled at the center of the north wall and logged at 1-min intervals during all experiments. The cross-calibration process is described in detail in the SI.

Room Air Temperature

Room air temperatures were measured with LittleFuse Model PR103J2 ultra-precision interchangeable thermistors that were mounted on 10 poles around the room (Figure 1) and have a nominal accuracy of ±0.05 ºC. The sensors were housed within radiation shields with openings to promote airflow past the sensors. There were 20 thermistors at the start of experiments and 14 by the end, with the other six becoming inoperable or disconnected through the study.

Hot Sphere Anemometers

Air speeds and temperatures were measured using SensoAnemo 5100SF transducers with omnidirectional (spherical) air speed sensors as part of the AirDistSys 5000 measurement system (Sensor-Electronic, Gliwice, Poland). The probes measure velocity vector magnitudes for air speeds from 0.05–5 m s^{-1} with an accuracy of ±0.02 m s^{-1} or ±1% of the readings. Up to eleven probes were deployed in each experiment in several different configurations. Figures 1a and 1b show the configurations used for 11 experiments each in the meeting and classroom, in which the sensors were arranged along the N-S transect of the room at three heights. Configurations used in other meeting room experiments are shown in SI figures. In most of those other experiments, seven of the sensors were placed at varied heights on a single pole to look at the vertical profile in one location, two were placed at two heights above a manikin, and two were placed inside the window that was covered on the outside with insulation.

Sequences of Events

The sequence of events varied across experiments, but all included a preparation phase, a period of constant tracer release, and a post-release interval of steady HVAC operation. Preparation included the following elements: mix as needed to approach or achieve uniform CO_2 at all room measurement points and ideally throughout the chamber; ventilate and heat or cool the chamber as needed to set the starting room CO_2 and temperature conditions to be within the range of those encountered in occupied spaces and to enable accurate measurements as CO_2 or temperature changes during the experiment; prime the supply air heating or cooling coils; set the supply airflow and outdoor air fraction, and thus the air exchange rate(or leave both off for no AHU conditions); and reduce particle concentrations for experiments that included particle release. Pre-experiment, the air was mixed and filtered using some combination of the chamber HVAC system and the four PACs. As needed, outdoor air gas supplied to reduce CO_2 by increasing the outdoor air fraction and/or opening the exterior door. The precise timing of each preparation element varied. During the preparation phase, researchers moved around the room to start and then stop the PACs and in some cases to move the location of the HVAC return air opening. The HVAC system was set to experimental conditions and human movement stopped in the chamber at least 10 min before each release to allow baseline airflow patterns to be established. After the

test conditions were set, there was a release of CO_2 and sometimes a co-release of particles. Following the release, airflow and supply air temperature conditions were maintained to observe the evolution of tracer concentrations for a defined post-release interval. Tracers were released using the apparatus described above, in the quantities and over the durations noted in Table 1. The interval over which conditions were maintained after the end of the release varied from roughly 10 min up to 30 min or more. We note that spatially resolved temperatures changed through the course of each experiment with heated or cooled supply air.

Analysis of Tracer Data

Analyses of impacts were based on the increases in concentrations above baseline during and following each tracer release. While analyses were conducted for all CO_2 measurement points in the room, the most important exposure results are based on measurements at the heads of the thermal manikins. The actual or observed increases ($C_{a,i}$) were calculated by subtracting the projected baseline concentration ($C_{b,i}$) that would have occurred if there had been no emission event from the measured concentration ($C_{m,i}$) at each location i:

$$C_{a,i}(t\ = C_{m,i}(t)\ -\ C_{b,i}(t) \quad (1)$$

We focus on baseline-subtracted concentrations because many experiments were conducted without returning the chamber to a starting condition of outdoor CO_2 levels.

The time-integral of the above-baseline increase at each location gives the simulated exposure concentration ($X_{a,i}$) for the release:

$$X_{a,i} = \int_{t_0}^{t_{end}} C_{a,i}(t)dt \quad (2)$$

This exposure period began with the start of the release (t_0) and ended after a post-release interval of at least 15 minutes, or as long as conditions in the room remained unchanged following the release if less than 15 minutes (t_{end}). The post-release period was included to account for delays of several minutes for the tracer plume to mix to all parts of the room and also to account for a typical exposure scenario where occupants remain in a room after a speaker finishes.

Baseline CO_2 Projection

At each location, $C_{b,I}$ was projected from just before the release to the end of the post-release period. This baseline was spatially and temporally dynamic, depending on the airflow conditions for the room and whether the chamber returned to the starting condition of outdoor CO_2 levels between experiments. For experiments with well mixed conditions at the start, the baseline projection of CO_2 for each location was similar; if the cell was not well mixed, then baseline projections varied by location. A brief summary of how baseline projections were determined is included here, with more details provided in the SI.

For the 29 experiments without intentional outdoor air, the outdoor air exchange was considered to be zero with no loss of CO_2 from the cell. Fitting a first order decay model to the measured concentrations in seven of these experiments that had adequate mixing and a long enough interval after the release found a mean air exchange rate of 0.08 and range of -0.03 to 0.19 h^{-1}. When measurements around the room prior to a release indicated well mixed conditions throughout the cell, the initial concentration at each measurement point was used as the baseline for the experiment, at that location. When the researcher was present during the experiment, a

steady CO_2 release rate of 0.23 LPM was included and assumed to be instantaneously mixed in the room [72]. If the observed concentration increase in the room indicated that CO_2 from the prior emission event had not fully mixed throughout the *cell* before the next release, it was assumed that the baseline CO_2 concentration at each location would decrease by first order decay from the concentration measured at the location just before the release to the expected concentration for a perfectly mixed cell. The decay would not actually be first order as air coming into the room from the plenum would have a steadily increasing concentration as the CO_2 mixed into the plenum, but the error of treating it as first order are small.

For all experiments with intentional ventilation, the room and plenum were well mixed at the beginning of each release (t_0). Baseline concentrations at each location were expected to decrease by first order decay (at rate λ) from the initial uniform concentration just before the release ($C_{0,i}$) toward the estimated steady-state background, accounting for both entry from outdoors (C_{out}) and emissions from the researcher if present in the room (E_R) [73]:

$$C_{b,i}(t) = C_{0,i}exp(-\lambda t) + (\frac{E_R}{\lambda V} + C_{out})[1 - exp(-\lambda t)] \quad (3)$$

Estimation of Perfectly-Mixed Concentration

To provide a consistent reference value to assess the quality of mixing across experiments, we used a single-zone mass balance model to calculate the time-dependent, theoretical, perfectly-mixed concentration in the *cell* (room plus plenum) resulting from the CO_2 released in each experiment. These calculations assumed that released CO_2 was instantaneously mixed through the cell. Strictly, the open plenum above the ceiling and the room below are separate zones that are connected by the AHU and by the open ceiling panel; air leaves the two-zone system via the exhaust air damper in the plenum and outdoor air is supplied to the room. Even so, comparing the observed concentrations at various locations within the room to those that would occur if the cell were instantly and perfectly mixed provides a quantitative indication of the extent of mixing.

For all experiments, the perfectly-mixed background ($C_{b,T}$) and release period (C_T) CO_2 concentrations were determined. Without intentional outdoor air ventilation, C_T would increase linearly with CO_2 emission from the controlled release at a rate of (E_T/V) and exhalation by the researcher (E_R). For experiments with intentional ventilation, the theoretical well-mixed concentration resulting from a metered release was calculated using an alternate form of Equation 3, with different emission terms for the release and post-release interval (see SI).

As detailed in the SI, the incremental, perfectly-mixed exposure (X_T) was calculated using the time integration of baseline-subtracted concentrations over the same release (t_0) and post-release interval (t_{end}) as was used in Equation 2 to determine $X_{a,i}$:

$$X_T = \int_{t_0}^{t_{end}} [C_T(t) - C_{b,T}(t)]dt \quad (4)$$

For each measurement location, an Exposure Relative to perfectly Mixed (ERM) metric was calculated as the ratio of the time-integrated observed concentration to the integral of the theoretical concentration that would have resulted from the actual emission rate and duration if the chamber were completely and instantaneously mixed:

$$ERM_{a,i} = \frac{X_{a,i}}{X_T} \quad (5)$$

We present the ERM with appreciation and acknowledgement of the seminal works of Sandberg[60] and Sandberg and Sjoberg[74] that present ventilation efficiency and air of air and

provide methods to determine these parameters and related metrics for various source release patterns. In the current paper we specify and use ERM to present the impacts of inefficient ventilation from the perspective of room occupants at various discrete locations.

Results

Impact of Supply Air on Thermal Stratification

The effect of the HVAC supply on vertical mixing in the room is indicated by the patterns of mean air temperature with height, as shown in Figure 2. During heating, warm air exiting the ceiling registers did not mix down into the breathing zone of the room. Rather, the warm supply air remained near the ceiling and was later drawn into the exhaust plenum, leading to thermally stratified conditions.

In the meeting configuration, stratification during heating was similar with four or two supply registers open, despite the latter having higher supply air velocities, and with or without 20% OA, which is not expected to impact stratification. Temperatures were generally vertically uniform when supply air was cooled or unconditioned, and also when there was no mechanical airflow, as heat released by the thermal manikins, researcher when present, electronic equipment, and southern wall added enough energy to induce mixing. The right panel of Figure 2 shows that temperatures at the southern wall tended to be a bit higher than elsewhere in the room at the same height.

Under the classroom setup with two uninsulated window sections, the vertical temperature profiles differed from those observed in the meeting room with all windows covered. In classroom experiments, temperatures at 91 and 183 cm height were very similar during both heating and cooling. With cooled supply air, temperatures at the bottom of the classroom were slightly lower than those at 91 cm; this is in contrast to the meeting room, where temperatures were the same at 91 cm and below under cooling conditions.

The radiative heat gains from the two windows not covered with insulation were in the range of 170–580 W, but the window blinds that were set to block direct radiative heating of the room caused a temperature increase of the air just inside the windows relative to the general room to 1.5–3.5 ºC (right panel of Figure 2).

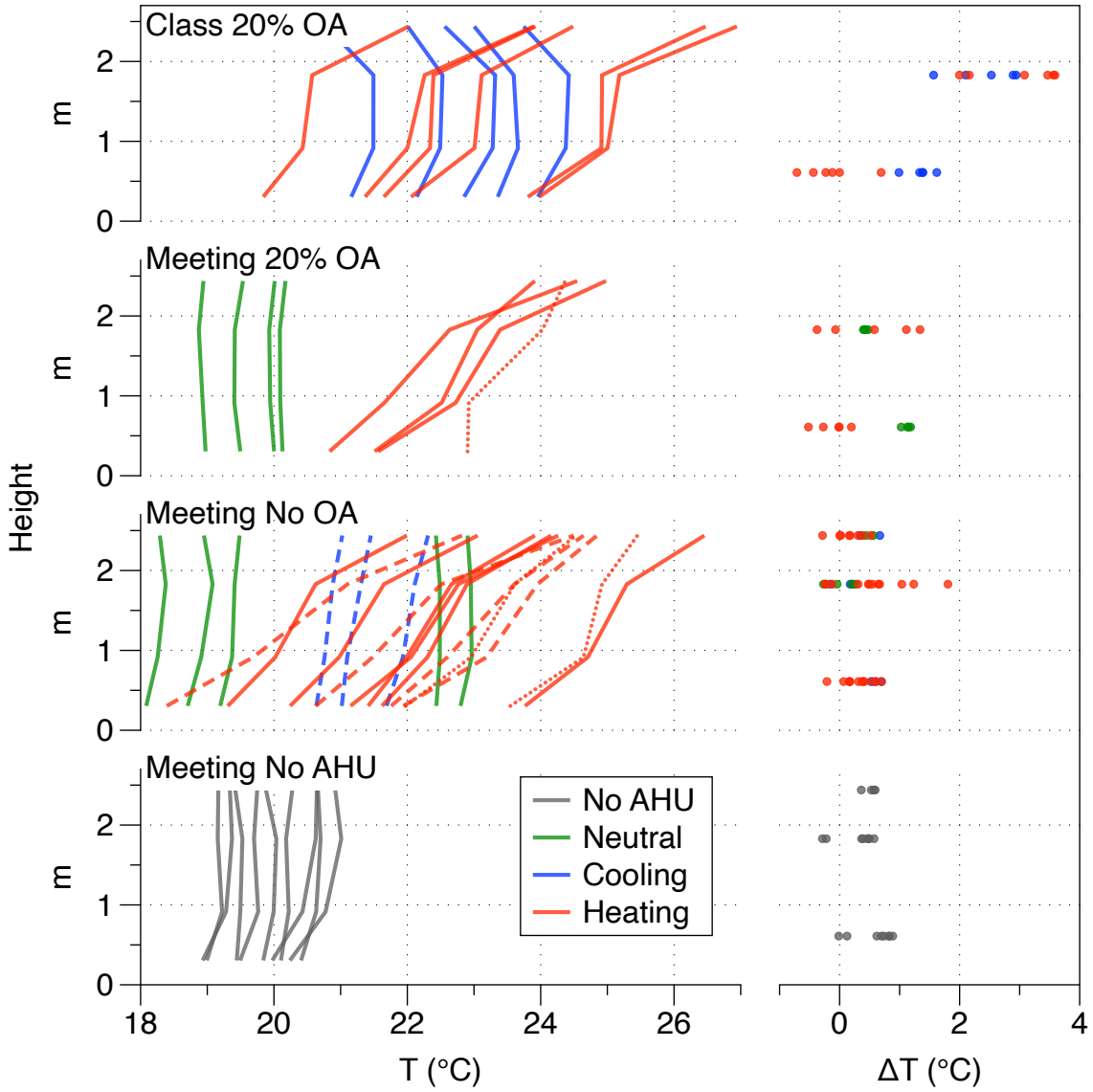

Figure 2. Vertical temperature profiles by configuration and supply air condition. Left panel presents mean temperature across all sensors at each height, as indicated in Figure 1, and excluding sensors at the southern wall and window; solid lines show experiments with four diffusers open, hatched lines are experiments with two diffusers covered and two open, and dotted lines show experiments with one or two portable air cleaners operating. The right panel shows differences between the southern wall / window and the room.

Illustrative examples of the differences in temperature patterns along the south to north axis of the room are presented in Figure S12 for the meeting room with no AHU, neutral, and heating supply air, and in Figure S13 for the classroom under cooling and heating supply conditions.

In the meeting configuration, temperatures were close to uniform vertically and along the N-S transect when there was no AHU or neutral temperature supply air. With heating, there was a clear vertical stratification and temperatures were slightly higher at the south end, just inside the insulated windows and above the exterior wall (Figure S12, Figure 2).

In the classroom, heating also caused stratification, with the highest temperatures at the top of the room but similar temperatures at one-third and two-third heights of the room (Figure S13, Figure 2). The air adjacent to the uncovered windows was substantially warmer than other places in the room at the same height.

Consistent with the observed temperature stratification, substantially lower air speeds were recorded in the room during heating conditions compared to neutral or cooling supply flows. Figure S14 presents air speeds at nine locations in each of four experiments. With heating in the meeting room, air speeds of 0.10–0.15 m s^{-1} were measured in three of five locations in the upper half of the room and the other two upper half locations and all four in the lower half of the room had air speeds ≤0.06 m s^{-1}. Heating in the classroom with uncovered windows produced air speeds ≤0.06 m s^{-1} in almost all measured locations throughout the room and a few >0.10 m s^{-1} occurring adjacent to the uninsulated, uncovered window. Air speeds were higher with neutral airflow under both room configurations, with all measurements >0.05 m s^{-1} and more than half >0.10 m s^{-1}. When cooled air was supplied in the classroom, air speeds exceeded 0.10 m s^{-1} at all locations and 0.15 m s^{-1} at most locations, with the exception of the upper part of the window.

Impact of Stratification on Dispersion of Aerosols from Speaking

The limited vertical mixing under stratified conditions led to elevated concentrations of CO_2 in the breathing zone. This is shown clearly in Figures 3 and 4, which present summary statistics for ERMs by vertical level, excluding sensors within 2 m of a release. Summary results are provided at the manikin level for each experiment in Table 1.

Figure 3 shows ERM distributions for the meeting room experiments without OA, by supply air condition. Cooled or neutral supply air led to good mixing of the simulated speaking emissions and low variability in the concentrations at each room height. ERMs under these conditions were close to unity because mixing extended into the plenum. With the AHU off, mixing induced by the thermal manikins and equipment in the room was sufficient to avoid stratification. However, there was substantially more variability than with mechanical mixing, with many cases of ERMs >1.0 as there was less air exchange with the plenum. Stratification when supply air was heated resulted in lower concentrations in the top part of the room and higher and more varied concentrations at the manikins. Differences in ERMs calculated for the manikins and the vertical middle of the room likely resulted more from their horizontal proximity to sources than their slightly different heights, as the "Middle" CO_2 sensors were in the corners. Median ERMs at the manikin level were approximately twice as high with heating as they were with cooling or neutral air distribution. The range of values was also much larger, with heating ERMs at several locations exceeding 5.0 whereas all ERMs for cooling and neutral supply were <1.5. Median levels in the lower and breathing zone sections of the room were similar for heating, cooling and neutral airflow, but heating resulted in much higher ERMs at some locations.

Figure 4 shows analogous data for experiments conducted in the meeting and classroom under conditions of 20% OA, with the same supply air flow rates used in meeting room experiments without OA. The basic results with OA were the same: ERMs again were more uniform with cooling or neutral temperature supply air compared to heating. During heating, ERMs varied at each height in the room, as indicated by the broad boxes and whiskers. Heating ERMs also were more variable between heights, with the lowest CO_2 at the top of the room, higher CO_2 in the middle and lower heights, and the highest CO_2 at the manikin level.

Importantly, ERMs with 20% OA were uniformly higher than those without OA, meaning there was a greater difference between the observed exposures and those that would have resulted with complete mixing. This is because ventilation with OA and perfect mixing theoretically should result in lower concentrations, which sets lower values in the denominator of the ERM equation. With poor mixing, the supplied outdoor air does not effectively dilute and remove the tracer emitted in the breathing zone. With heating in the ventilated room experiments, stratification caused at least 25% of the manikins to have exposures 2.5 times those that would have occurred with perfect mixing. These results are similar to those reported in prior studies of stratification with heating [57,58]. Manikin exposures were also higher than ideal, well-mixed conditions when the meeting room was ventilated with neutral temperature air and the classroom was ventilated with cooled air. The result necessarily indicates imperfect mixing, almost certainly related to delayed mixing in the plenum. For cooling in the classroom, the available temperature data suggest short-circuiting as some cooled air moved from the supply diffusers across the ceiling directly to the return opening, consistent with observed cooler temperatures at the top of the room in the top panel of Figure 2 and the cooler temperatures at the top of the northern half of the room in the bottom two panels of Figure S13.

Mixing with Portable Air Cleaners

Figures 3 and 4 show that within-zone mixing fans—in these experiments provided by portable air cleaners—can increase mixing enough to avoid the negative impacts of stratification. In the meeting room setup without OA ventilation, the operation of two PACs during two heating experiments provided adequate mixing to produce vertically uniform ERMs that were very close to 1.0, like those with neutral temperature supply. In the meeting room with 20% OA, operation of a single air cleaner during heating resulted in similar ERM as neutral temperature supply air.

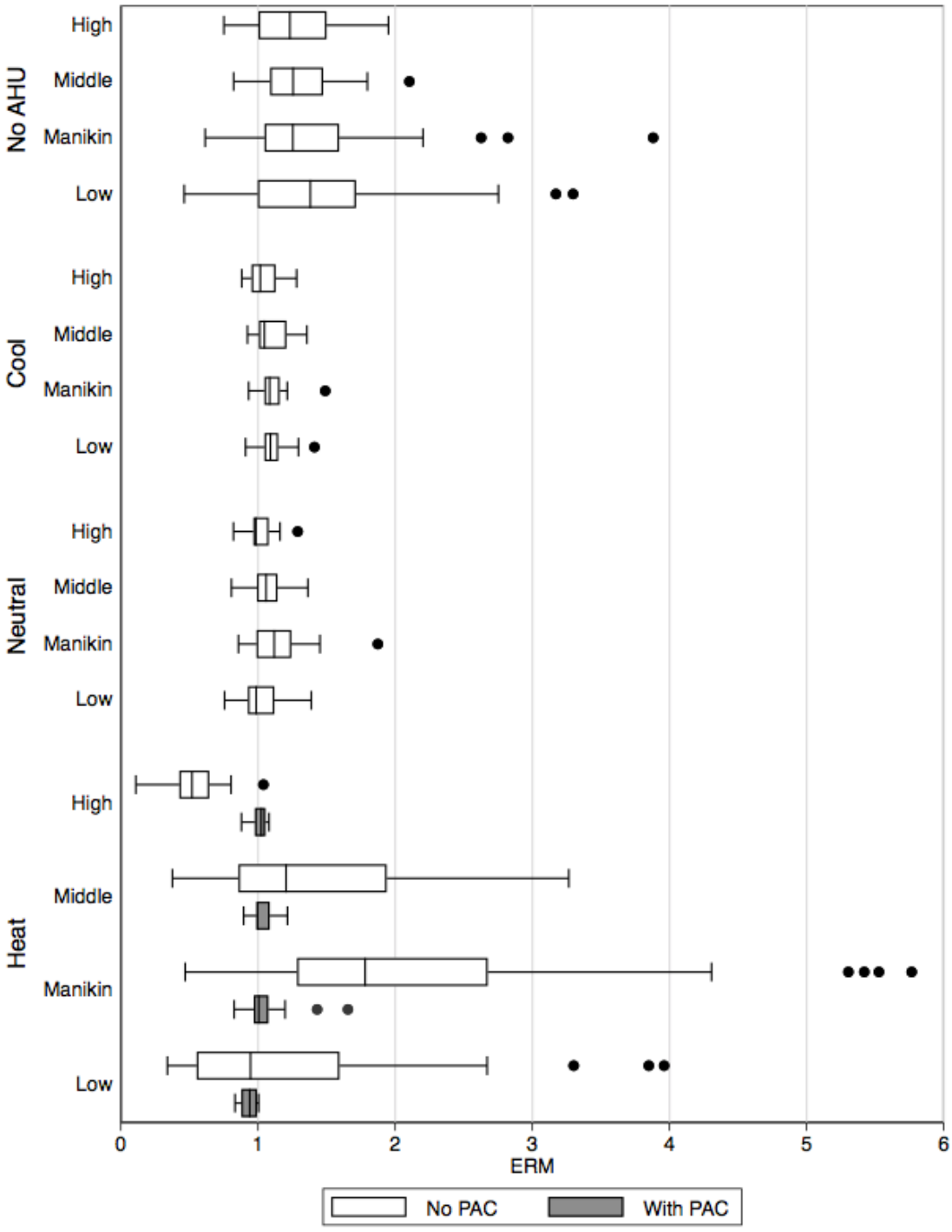

Figure 3: Exposures Relative to perfectly Mixed (ERM) at each vertical level of the room under each HVAC condition in the meeting room experiments with no outdoor air. ERMs as calculated by Equation 5. Boxes show median and interquartile range (IQR) and whiskers extend to 1.5× IQR. Measurement heights: Low = 30 cm; manikins mostly seated at 105 cm, standing teacher at 121 cm; middle = 137 cm; High = 244 cm.

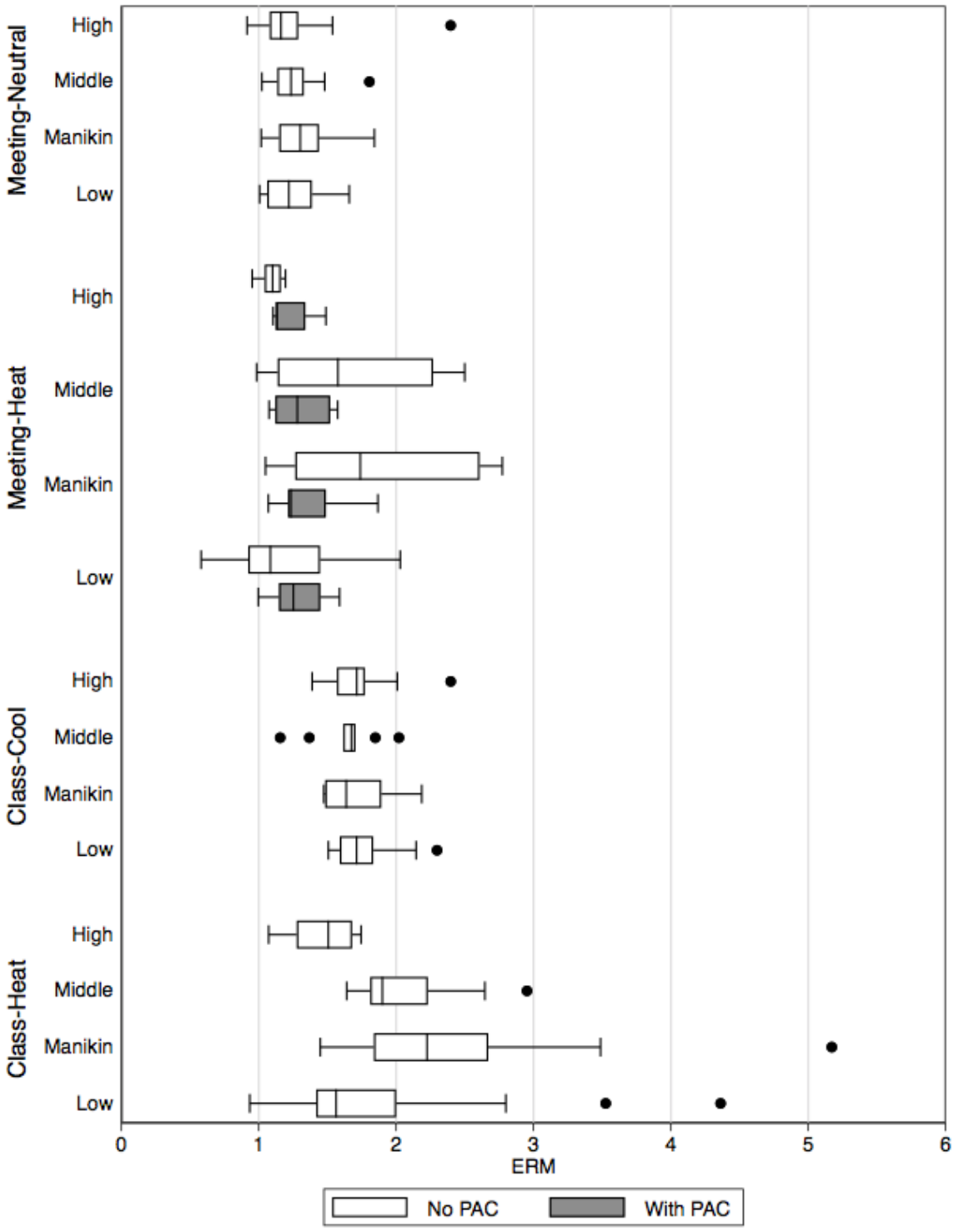

Figure 4: Exposures Relative to perfectly Mixed conditions at each vertical level of the room under each HVAC condition in the meeting and classroom experiments with 20% outdoor air. Details as described in caption to Figure 3.

Impacts of HVAC and Proximity to Release on Exposure Patterns

Experiments were configured to explore the impacts of release location, two vs. four overheard diffusers, and location of the plenum return opening. While systematic reporting of these factors is beyond the scope of this paper, several examples are provided to illustrate key points.

The first example is shown in Figure 5, which presents the baseline-subtracted, time-resolved concentrations around the room during and following releases from just above the head of the manikin seated at the West position in the meeting. The conditions were: (a) no forced air, and air supplied at (b) neutral, (c) cooling, or (d) heating temperatures. Releases were 19.1–20.3 min each and conditions were maintained for another 20 min. Supply air was provided through NW and SE diffusers only (others were covered) and the return was in the NE corner. With cooling or neutral airflow, the tracer quickly mixed and there were no "hot spots" of substantially higher exposure. Without the AHU, the highest concentrations were at the middle-height sensor, 1.9 m away from the release horizontally and 15 cm higher. Stratification with heating caused substantially higher exposures at all locations between the release point and the return.

As shown in Figure 6, much larger spatial variations around the meeting room occurred following releases from the North manikin at standing height, with heating provided through four diffusers and the return at the CTR or NE position. While substantial differences were observed between the two experiments shown in the figure, especially the timing of the peak at the West manikin position, the spatial variations around the room were remarkably similar. In both cases, the highest concentrations and exposures occurred at the East and West manikins, which had ERMs of 3.1 and 5.2 for CTR return, and 3.9 and 5.7 for NE return. It took over five minutes for the plume to arrive at all five of the breathing zone measurement points in the southern part of the room, and almost 10 min to arrive at the SE corner. Exposures at these locations were only 0.7–1.8 relative to well-mixed.

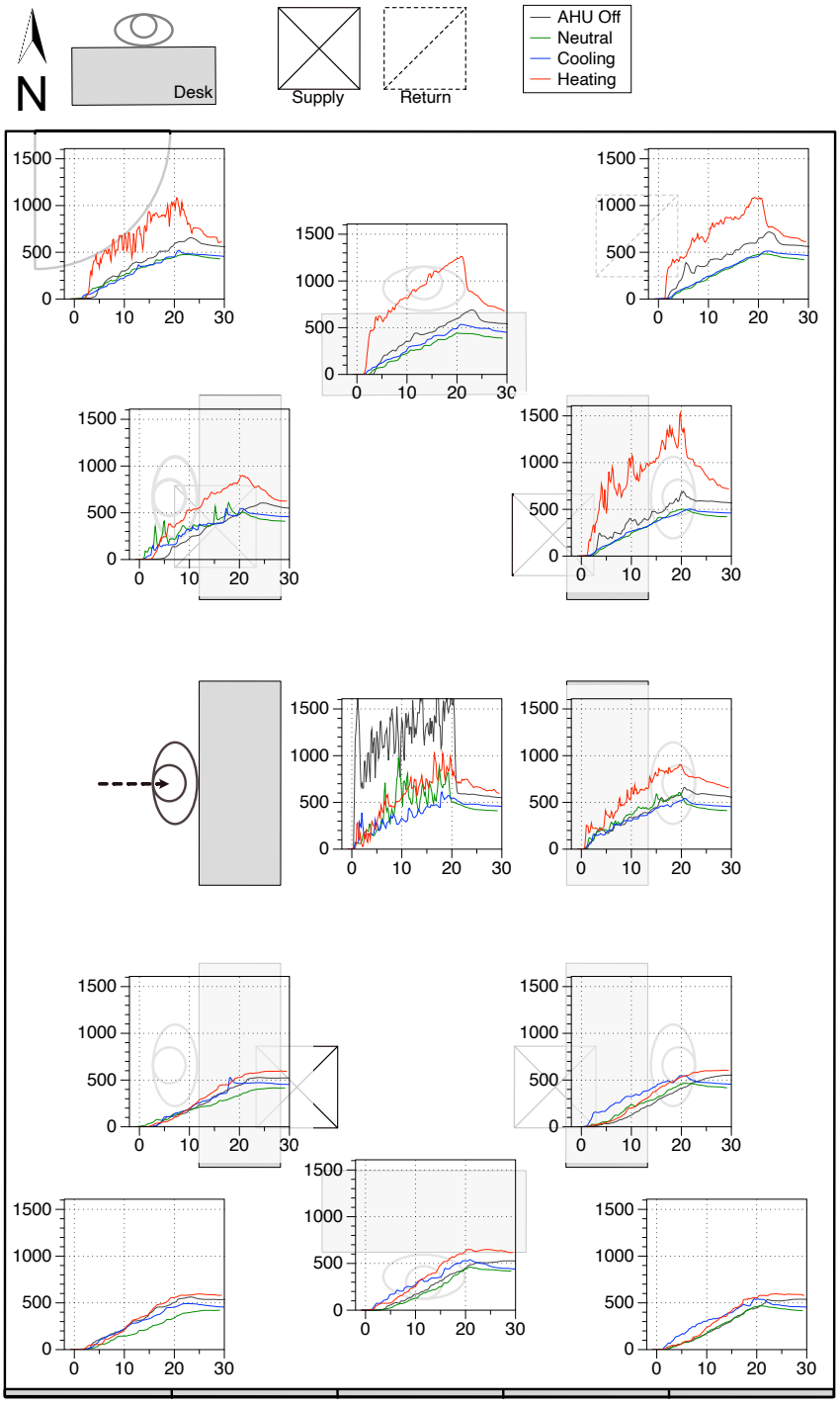

Figure 5. Baseline-subtracted, time-resolved concentrations during and following releases under varied air supply conditions in Meeting configuration. Tracer released at standing height at location indicated. Supply air provided via SE and NW diffusers with plenum connection at NE, as shown. Legend indicates supply air conditions.

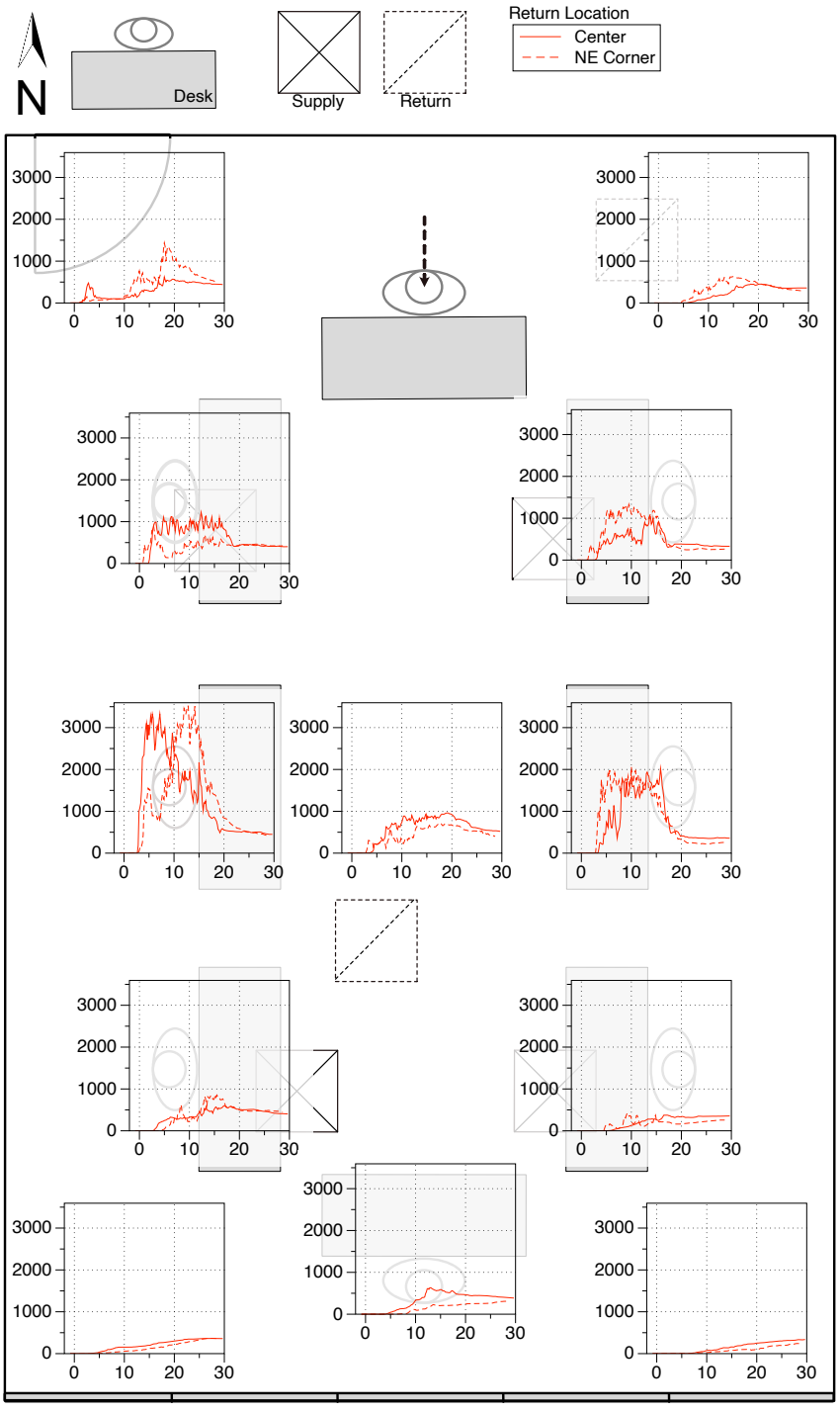

Figure 6. Baseline-subtracted, time-resolved concentrations during and following releases with heated supply from four diffusers and connection to plenum return in NE or Center, Meeting room.

Discussion

Impact of Poor Mixing on Effectiveness of Ventilation and HVAC Filtration

As detailed above, the CO_2 tracer gas from these experiments is assumed to be a good proxy for respiratory aerosol with diameters under 5 μm. To elucidate the importance of effectively moving air from the breathing and expiratory emission zone in the middle of the room into the HVAC system to achieve the benefits of ventilation and central HVAC filtration, Table 2 provides ratios of perfectly mixed concentrations with 20% OA and varied filtration efficiencies to the exposure that would occur with perfect mixing and no ventilation. The calculated results include the cases studied experimentally: a 15 or 30 min emission event followed by 15 min post-release occupancy, and also a 15 min emission event with 30 min post-occupancy interval. As noted in prior studies[34], effective filtration in the HVAC system can dramatically reduce exposures to indoor generated pollutants, even when the OA ventilation rate is limited. Ventilating with 20% OA and using a 50% efficient filter would reduce exposures in a well-mixed room by about 40–50% relative to no ventilation for the three release and post-release intervals examined. The target ERM to fully realize the benefits of ventilation and central filtration is 1.0.An ERM of 2 would negate this benefit of ventilation and filtration and an ERM of 4 translates to exposures that are twice as high as no ventilation or filtration.

Table 2. Calculated benefits of ventilation and filtration, assuming instantaneous and perfect mixing; exposure relative to the same conditions with no outdoor air ventilation and no filtration. Results based on total supply airflow of 18 cmh m^{-2} floor area and 0.86 ach.

Release + post occupancy (min)	20% OA					100% OA
	No filter	20% filter	50% filter	80% filter	95% filter	
15+15	0.85	0.75	0.63	0.54	0.50	0.49
30+15	0.78	0.63	0.52	0.44	0.40	0.40
15+30	0.82	0.76	0.58	0.45	0.40	0.35

Relevance to Controls for Airborne Transmission Risk Reduction in Buildings

The HVAC configuration used in the experiments reported here represents equipment in many US commercial buildings, but the extent to which study results were dictated by the specific supply registers, their arrangement in the room, and the airflows used is not known. The meeting room was configured to be representative of internal spaces with limited driving forces at any boundary and the classroom was used to explore a configuration in which the windows could have a substantial impact on heat transfer and mixing. However, the relatively mild outdoor temperatures and clear, sunny days from these experiments represent only a small fraction of winter conditions. While the movement of CO_2 is a proxy for small respiratory aerosol dynamics, it is important to recognize that airborne viruses also may be transferred via larger aerosol particles that behave differently and warrant study. The tracer was released at a continuous rate in the range of time-averaged expiratory flows reported for human speech, but dramatic coughing or sneezing events were not considered. The potential effect of a face covering on the near-field, momentum-driven trajectory of respiratory emissions was not examined in the present study. However, the findings of elevated concentrations in the vertical middle of the room

resulting from stratification should be relevant to scenarios in which a speaker is masked, as bulk air movements are more important than expiratory momentum in driving exposures across the room. Finally, of potentially great importance to the question of mixing within the breathing zone, there was no human movement in the room during the experiments, which would tend to mix the room more quickly than measured in the present study.

Conclusions

This study provides quantitative estimates of the hazards resulting from stratification and poor mixing in rooms heated with overhead HVAC, measured under realistic conditions. Under these conditions, the intended ventilation and filtration benefits from the central HVAC system may not be achieved and some individuals within the room may at times be exposed to respiratory aerosols emitted by someone else in the room at rates that are 5–6 times those that would occur under truly well-mixed conditions. This result demonstrates that poor mixing and low ventilation effectiveness resulting from stratification can be problematic even in rooms arranged to maintain >2 m distance between all occupants. The inclusion of a broad range of experiments—using two room configurations with realistic numbers of simulated occupants, variations in the locations of HVAC supply and return, and with and without window effects—established the robustness of these findings.

When an overhead HVAC system is in heating mode, it is important to add mechanical mixing to avoid stratification. Eliminating stratification is particularly important to ensuring that the benefits of outdoor air ventilation and central filtration are achieved in the room. While mixing coule be provided by portable fans, PACs provide substantial additional benefit by filtering as well as mixing the air and their use is recommended.

Acknowledgements

This research could not have been done without the outstanding logistics support provided by the FLEXLAB team of Sarah Daniel, Rod Mobini, Stacy Curry, Ari Harding, and Cindy Regnier.

Funding:

This research was supported by the U.S. Department of Energy Office of Science, through the National Virtual Biotechnology Laboratory, a consortium of DOE national laboratories focused on response to COVID-19, with funding provided by the Coronavirus CARES Act. The use of FLEXLAB in this work was supported by the Building Technologies Office, within the DOE's Office of Energy Efficiency and Renewable Energy, under Contract DE-AC02-05CH11231.

Conflict of Interest

All authors confirm no conflicts of interest.

Author Credits:

Brett C. Singer: Funding Acquisition (supporting), Conceptualization (lead), Methodology (lead), Investigation (lead), Project Administration (lead), Formal analysis (supporting), Writing – Original Draft Preparation (lead), Writing – Review and Editing (lead), Supervision (lead).

Haoran Zhao: Investigation (lead), Data curation (lead), Formal analysis (lead), Writing – Original Draft Preparation (supporting), Visualization (lead).

Chelsea V. Preble: Investigation (lead), Data curation (supporting), Writing – Original Draft Preparation (supporting), Writing – Review and Editing (lead).

William W. Delp: Conceptualization (supporting), Methodology (supporting), Data curation (lead), Formal analysis (lead), Visualization (lead).

Jovan Pantelic: Conceptualization (lead), Methodology (lead), Investigation (lead), Writing – Original Draft Preparation (supporting), Visualization (supporting).

Michael D. Sohn: Funding Acquisition (supporting), Methodology (lead), Investigation (supporting), Project Administration (supporting), Writing – Review and Editing (supporting), Supervision (supporting).

Thomas W. Kirchstetter: Funding Acquisition (lead), Project Administration (lead), Writing – Review and Editing (supporting), Supervision (supporting), Investigation (supporting).

Table 1. Details of experiments.

ID	Supply condition	Diffu-sers	Return	Supply air flow (cmh)	Outdoor air flow (cmh)	OA frac.	Supply air T (ºC)	SAT–RAT (ºC)	Location, height (cm)	Release heated	Researcher in room	Release start time	Release duration (min)	Manikin ERM mean (min-max)
1203A	No AHU	NA	NE	7	4	NA	17.5	NA	E, 109	N	N	13:53	16.38	1.5 (0.6–3.8)
1203C	No AHU	NA	NE	5	16	NA	18.9	NA	N, 109	N	N	15:15	14.70	1.5 (0.8–2.6)
1204A	No AHU	NA	Center	3	7	NA	19.5	NA	N, 109	Y	N	15:56	13.80	1.4 (1–1.9)
1204B	No AHU	NA	Center	4	10	NA	15.3	NA	N, 109	Y	N	16:38	11.97	1.5 (1.1–2.1)
1207A	No AHU	NA	Center	5	14	NA	14.4	NA	N, 154	Y	N	12:26	14.10	1.6 (0.9–2.8)
1217A	No AHU	NA	NE	7	11	NA	19.0	NA	N, 154	Y	Y	15:40	19.90	1.4 (1.1–1.7)
1201C	No AHU	NA	SW	2	5	NA	16.5	NA	W, 109	N	N	16:49	14.33	1.3 (0.9–2.2)
1201D	No AHU	NA	SW	2	8	NA	17.2	NA	W, 109	N	N	17:20	14.53	1.2 (0.9–1.8)
1214B	No AHU	NA	NE	11	57	NA	28.2	NA	W, 154	Y	Y	19:40	20.28	1.2 (1–1.4)
1208B	Cool	2	NE	1015	12	0.01	14.0	-6.9	N, 154	Y	N	13:19	15.42	1.1 (1–1.5)
1208D	Cool	2	SW	1005	16	0.02	17.0	-5.4	N, 154	Y	N	15:23	15.33	1.0 (0.9–1.2)
1216C	Cool	2	NE	981	16	0.02	15.5	-6.1	W, 154	Y	Y	19:20	19.90	1.1 (1–1.2)
1125A	Neutral	4	NE	1070	12	0.01	21.8	0.1	W, 109	N	N	12:45	30.40	1.3 (1.1–1.9)
1125B	Neutral	4	SW	1081	11	0.01	22.1	0.0	W, 109	N	N	14:09	29.00	1.2 (1–1.4)
1215A	Neutral	2	NE	1056	41	0.04	17.5	-0.1	W, 154	Y	Y	13:06	19.12	1.1 (0.9–1.3)
1215B	Neutral	2	NE	997	35	0.04	18.1	0.0	W, 154	Y	Y	13:56	19.20	1.0 (0.9–1.3)
1215C	Neutral	2	SW	1009	34	0.03	18.4	-0.1	W, 154	Y	Y	15:00	21.22	1.1 (1–1.3)
1203B	Heat	4	NE	1050	12	0.01	30.2	10.5	E, 109	N	N	14:30	14.28	1.4 (0.5–3.5)
1203D	Heat	4	NE	1038	11	0.01	31.6	10.6	N, 109	N	N	15:50	15.95	2.4 (1.3–3.4)
1203E	Heat	4	Center	1072	11	0.01	32.6	10.2	N, 109	N	N	16:40	15.17	2.5 (0.8–5.4)
1204C	Heat	4	Center	1061	19	0.02	31.2	9.1	N, 109	Y	N	17:42	14.97	2.1 (1.3–3)
1207B	Heat	4	Center	1067	13	0.01	31.5	9.4	N, 154	Y	N	13:33	14.73	2.4 (0.9–5.2)
1207C	Heat	4	NE	1059	13	0.01	33.1	8.8	N, 154	Y	N	15:48	13.73	2.5 (0.7–5.7)

1208A	Heat	2	NE	979	10	0.01	32.4	11.2	N, 154	Y	N	11:57	17.18	2.4 (1.0–6.6)
1208C	Heat	2	SW	979	10	0.01	32.2	10.4	N, 154	Y	N	14:25	9.48	2.6 (0.9–7.9)
1210A	Heat	2	SW	1046	20	0.02	30.0	6.6	N, 154	Y	N	18:41	15.95	1.6 (0.6–5.5)
1214A	Heat	2	NE	1035	9	0.01	31.8	11.6	W, 154	Y	Y	18:30	19.48	1.9 (1.3–2.8)
1215D	Heat[1]	2	NE	1064	13	0.01	33.6	11.6	W, 154	Y	Y	17:10	19.95	1.2 (0.8–1.7)
1215E	Heat[2]	2	NE	1039	17	0.02	34.6	11.2	W, 154	Y	Y	18:35	20.17	1.0 (1.0–1.1)
1218A	Neutral	4	NE	1047	200	0.19	17.5	-0.7	N, 154	Y	Y	14:58	14.47	1.3 (1.1–1.8)
1218B	Neutral	4	NE	1049	206	0.20	18.0	-0.7	N, 154	Y	Y	15:40	14.68	1.3 (1.0–1.8)
1218C	Neutral	4	NE	1058	218	0.21	18.3	-1.0	N, 154	Y	Y	16:50	15.32	1.4 (1.1–1.5)
1218D	Neutral	4	NE	1064	223	0.21	18.3	-1.2	N, 154	Y	Y	17:31	14.22	1.3 (1.2–1.4)
1216A	Heat	2	NE	990	212	0.21	30.5	9.0	W, 154	Y	Y	16:20	20.22	1.8 (1.0–2.7)
1216B	Heat	2	NE	1024	191	0.19	33.2	10.4	W, 154	Y	Y	17:50	20.42	1.9 (1.2–2.8)
1217B	Heat[3]	2	NE	1036	196	0.19	31.9	10.2	N, 154	Y	Y	17:30	20.08	1.3 (1.1–1.9)
1217C	Heat[4]	2	NE	1056	197	0.19	33.5	11.0	N, 154	Y	Y	18:59	20.53	1.7 (1.4–3.2)
1222D	Cool	4	NE	1008	189	0.19	16.7	-7.0	R1C, 109	Y	Y	12:35	14.83	1.7 (1.5–2.2)
1221B	Cool	4	NE	1003	184	0.18	14.8	-6.0	Teacher	Mid	Y	13:21	14.08	1.7 (1.5–2.0)
1222E	Cool[4]	4	NE	1025	188	0.18	16.4	-6.2	R1C, 109	Y	Y	14:05	15.33	1.6 (1.5–1.9)
1222F	Cool[4]	4	NE	1020	198	0.19	16.5	-5.5	R3W, 109	Y	Y	15:15	16.32	1.5 (1.2–1.8)
1221D	Cool[4]	4	NE	1024	207	0.20	15.7	-7.6	Teacher	Mid	Y	15:41	14.37	1.5 (1.3–1.9)
1222C	Heat	4	NE	1056	191	0.18	32.3	8.3	R1C, 109	Y	Y	11:35	14.98	2.2 (1.7–2.7)
1223B	Heat	4	NE	1095	207	0.19	29.9	8.0	R3W, 109	Mid	Y	10:50	14.95	2.3 (1.9–3.4)
1221C	Heat	4	NE	1041	206	0.20	31.7	8.1	Teacher	Mid	Y	14:25	14.78	2.2 (1.4–2.9)
1222B	Heat[4]	4	NE	1047	201	0.19	29.0	7.0	R1C, 109	Mid	Y	10:40	15.27	2.0 (1.7–2.2)
1223A	Heat[4]	4	NE	1054	201	0.19	26.9	6.9	R3W, 109	Y	Y	9:00	14.95	2.8 (1.7–5.1)
1222A	Heat[4]	4	NE	1056	207	0.20	29.4	7.9	Teacher	Mid	Y	9:10	14.83	1.9 (1.4–2.2)

[1] Two PACs were running on med flow during the experiment. [2] Two PACs were running on high flow during the experiment. [3] One PAC was running on high flow during the experiment. [4] A barrier was deployed in the room during the experiment.

Literature Cited

1. Morawska L, Tang JW, Bahnfleth W, et al. How can airborne transmission of COVID-19 indoors be minimised? *Environment International*. May 2020:105832.

2. Dietz L, Horve PF, Coil DA, Fretz M, Eisen JA, Wymelenberg KVD. 2019 Novel coronavirus (COVID-19) pandemic: Built environment considerations to reduce transmission. *mSystems*. 2020;5. April 28, 2020. https://msystems.asm.org/content/5/2/e00245-20. Accessed July 31, 2020.

3. Jones RM, Brosseau LM. Aerosol transmission of infectious disease. *Journal of Occupational and Environmental Medicine*. 2015;57:501–508.

4. Tang S, Mao Y, Jones RM, et al. Aerosol transmission of SARS-CoV-2? Evidence, prevention and control. *Environ Int*. 2020;144:106039.

5. Anderson EL, Turnham P, Griffin JR, Clarke CC. Consideration of the aerosol transmission for COVID-19 and public health. *Risk Analysis*. 2020;40:902–907.

6. Lindsley WG, Blachere FM, Davis KA, et al. Distribution of airborne influenza virus and respiratory syncytial virus in an urgent care medical clinic. *Clin Infect Dis*. 2010;50:693–698.

7. Yan J, Grantham M, Pantelic J, et al. Infectious virus in exhaled breath of symptomatic seasonal influenza cases from a college community. *PNAS*. 2018;115:1081–1086.

8. Milton DK, Fabian MP, Cowling BJ, Grantham ML, McDevitt JJ. Influenza virus aerosols in human exhaled breath: Particle size, culturability, and effect of surgical masks. *PLOS Pathogens*. 2013;9:e1003205.

9. Leung NHL, Chu DKW, Shiu EYC, et al. Respiratory virus shedding in exhaled breath and efficacy of face masks. *Nature Medicine*. 2020;26:676–680.

10. Lelieveld J, Helleis F, Borrmann S, et al. Model calculations of aerosol transmission and infection risk of COVID-19 in indoor environments. *International Journal of Environmental Research and Public Health*. 2020;17:8114.

11. Jones NR, Qureshi ZU, Temple RJ, Larwood JPJ, Greenhalgh T, Bourouiba L. Two metres or one: What is the evidence for physical distancing in Covid-19? *BMJ*. 2020;370:m3223.

12. Yang W, Elankumaran S, Marr LC. Concentrations and size distributions of airborne influenza A viruses measured indoors at a health centre, a day-care centre and on aeroplanes. *J R Soc Interface*. 2011;8:1176–1184.

13. Thatcher TL, Lai ACK, Moreno-Jackson R, Sextro RG, Nazaroff WW. Effects of room furnishings and air speed on particle deposition rates indoors. *Atmospheric Environment*. 2002;36:1811–1819.

14. Hinds WC. *Aerosol Technology: Properties, Behavior, and Measurement of Airborne Particles*. 2nd ed. New York: Wiley; 1999.

15. Yang W, Marr LC. Dynamics of airborne influenza A viruses indoors and dependence on humidity. *PLOS ONE*. 2011;6:e21481.

16. Kenarkoohi A, Noorimotlagh Z, Falahi S, et al. Hospital indoor air quality monitoring for the detection of SARS-CoV-2 (COVID-19) virus. *Science of The Total Environment*. 2020;748:141324.

17. Lednicky JA, Lauzardo M, Fan ZH, et al. Viable SARS-CoV-2 in the air of a hospital room with COVID-19 patients. *International Journal of Infectious Diseases*. 2020;100:476–482.

18. Santarpia JL, Rivera DN, Herrera V, et al. Aerosol and Surface Transmission Potential of SARS-CoV-2. *Scientific Reports*. 2020;10. July 29, 2020. https://doi.org/10.1038/s41598-020-69286-3. Accessed August 3, 2020.

19. Chia PY, Coleman KK, Tan YK, et al. Detection of air and surface contamination by SARS-CoV-2 in hospital rooms of infected patients. *Nature Communications*. 2020;11:1–7.

20. Liu Y, Ning Z, Chen Y, et al. Aerodynamic analysis of SARS-CoV-2 in two Wuhan hospitals. *Nature*. 2020;582:557–560.

21. Lednicky JA, Shankar SN, Elbadry MA, et al. Collection of SARS-CoV-2 virus from the air of a clinic within a university student health care center and analyses of the viral genomic sequence. *Aerosol and Air Quality Research*. 2020;20:1167–1171.

22. Horve PF, Dietz L, Fretz M, et al. Pre-print: Identification of SARS-CoV-2 RNA in Healthcare Heating, Ventilation, and Air Conditioning Units. June 2020. June 28, 2020. https://www.medrxiv.org/content/10.1101/2020.06.26.20141085v1. Accessed July 31, 2020.

23. van Doremalen N, Bushmaker T, Morris DH, et al. Aerosol and surface stability of SARS-CoV-2 as compared with SARS-CoV-1. *N Engl J Med*. 2020;382:1564–1567.

24. Fears AC, Klimstra WB, Duprex P, et al. Persistence of severe acute respiratory syndrome coronavirus 2 in aerosol suspensions. *Emerging Infectious Diseases*. 2020;2. September 2020. https://wwwnc.cdc.gov/eid/article/26/9/20-1806_article. Accessed August 28, 2020.

25. Shen Y, Li C, Dong H, et al. Community outbreak investigation of SARS-CoV-2 transmission among bus riders in eastern China. *JAMA Intern Med*. September 2020. September 1, 2020. https://jamanetwork.com/journals/jamainternalmedicine/fullarticle/2770172. Accessed October 6, 2020.

26. Miller SL, Nazaroff WW, Jimenez JL, et al. Transmission of SARS-CoV-2 by inhalation of respiratory aerosol in the Skagit Valley Chorale superspreading event. *Indoor Air*. September 2020.

27. Hwang SE, Chang JH, Oh B, Heo J. Possible aerosol transmission of COVID-19 associated with an outbreak in an apartment in Seoul, South Korea, 2020. *International Journal of Infectious Diseases*. 2021;104:73–76.

28. Lu J, Gu J, Li K, et al. COVID-19 outbreak associated with air conditioning in restaurant, Guangzhou, China, 2020. *Emerg Infect Dis*. 2020;26:1628–1631.

29. Park SY, Kim Y-M, Yi S, et al. Coronavirus disease outbreak in call center, South Korea. *Emerg Infect Dis*. 2020;26:1666–1670.

30. Yu ITS, Li Y, Wong TW, et al. Evidence of airborne transmission of the severe acute respiratory syndrome virus. *New England Journal of Medicine*. 2004;350:1731–1739.

31. Buonanno G, Stabile L, Morawska L. Estimation of airborne viral emission: Quanta emission rate of SARS-CoV-2 for infection risk assessment. *Environment International*. 2020;141:105794.

32. Chen W, Zhang N, Wei J, Yen H-L, Li Y. Short-range airborne route dominates exposure of respiratory infection during close contact. *Building and Environment*. 2020;176:106859.

33. Bolashikov ZD, Melikov AK. Methods for air cleaning and protection of building occupants from airborne pathogens. *Building and Environment*. 2009;44:1378–1385.

34. Azimi P, Stephens B. HVAC filtration for controlling infectious airborne disease transmission in indoor environments: Predicting risk reductions and operational costs. *Build Environ*. 2013;70:150–160.

35. Kowalski WJ, Bahnfleth WP, Whitman TS. Filtration of airborne microorganisms: Modeling and prediction. *ASHRAE Transactions: Research*. 1999;105.

36. Sultan ZM, Nilsson GJ, Magee RJ. Removal of ultrafine particles in indoor air: Performance of various portable air cleaner technologies. *Hvac&R Research*. 2011;17:513–525.

37. First MW, Nardell EA, Chaissan W, Riley R. Guidelines for the application of upper-room ultraviolet germicidal irradiation for preventing transmission of airborne contagion—Part II: Design and operation guidance. *ASHRAE TRANSACTIONS*. 1999;105:CH-99-12-2.

38. Dumyahn T, First M. Characterization of ultraviolet upper room air disinfection devices. *American Industrial Hygiene Association Journal*. 1999;60:219–227.

39. Kujundzic E, Matalkah F, Howard CJ, Hernandez M, Miller SL. UV air cleaners and upper-room air ultraviolet germicidal irradiation for controlling airborne bacteria and fungal spores. *Journal of Occupational and Environmental Hygiene*. 2006;3:536–546.

40. Morawska L. Droplet fate in indoor environments, or can we prevent the spread of infection? *Indoor Air*. 2006;16:335–347.

41. Li Y, Leung GM, Tang JW, et al. Role of ventilation in airborne transmission of infectious agents in the built environment ? A multidisciplinary systematic review. *Indoor Air*. 2007;17:2–18.

42. Tang JW, Li Y, Eames I, Chan PKS, Ridgway GL. Factors involved in the aerosol transmission of infection and control of ventilation in healthcare premises. *Journal of Hospital Infection*. 2006;64:100–114.

43. Awbi HB. Air movement in naturally-ventilated buildings. *Renewable Energy*. 1996;8:241–247.

44. Tang JW, Nicolle A, Pantelic J, et al. Different types of door-opening motions as contributing factors to containment failures in hospital isolation rooms. Costa C, ed. *PLoS ONE*. 2013;8:e66663.

45. Eames I, Shoaib D, Klettner CA, Taban V. Movement of airborne contaminants in a hospital isolation room. *J R Soc Interface*. 2009;6. December 6, 2009. https://royalsocietypublishing.org/doi/10.1098/rsif.2009.0319.focus. Accessed March 9, 2021.

46. Bolashikov ZD, Melikov AK, Kierat W, Popiołek Z, Brand M. Exposure of health care workers and occupants to coughed airborne pathogens in a double-bed hospital patient room with overhead mixing ventilation. *HVAC&R Research*. 2012:15.

47. Beggs CB, Kerr KG, Noakes CJ, Hathway EA, Sleigh PA. The ventilation of multiple-bed hospital wards: Review and analysis. *American Journal of Infection Control*. 2008;36:250–259.

48. Cermak R, Melikov A. Protection of occupants from exhaled infectious agents and floor material emissions in rooms with personalized and underfloor ventilation. *HVAC&R Res*. 2007;13:23–38.

49. Pantelic J, Tham KW. Adequacy of air change rate as the sole indicator of an air distribution system's effectiveness to mitigate airborne infectious disease transmission caused by a cough release in the room with overhead mixing ventilation: A case study. *HVAC&R Research*. 2013;19:947–961.

50. Licina D, Melikov A, Pantelic J, Sekhar C, Tham KW. Human convection flow in spaces with and without ventilation: Personal exposure to floor-released particles and cough-released droplets. *Indoor Air*. 2015;25:672–682.

51. Pantelic J, Tham KW, Licina D. Effectiveness of a personalized ventilation system in reducing personal exposure against directly released simulated cough droplets. *Indoor Air*. 2015;25:683–693.

52. Pantelic J, Sze-To GN, Tham KW, Chao CYH, Khoo YCM. Personalized ventilation as a control measure for airborne transmissible disease spread. *J R Soc Interface*. 2009;6.

December 6, 2009. https://royalsocietypublishing.org/doi/10.1098/rsif.2009.0311.focus. Accessed August 3, 2020.

53. Qian H, Zheng X. Ventilation control for airborne transmission of human exhaled bio-aerosols in buildings. *Journal of Thoracic Disease*. 2018;10. July 2018. https://jtd.amegroups.com/article/view/18723. Accessed March 26, 2021.

54. Chao CYH, Wan MP. A study of the dispersion of expiratory aerosols in unidirectional downward and ceiling-return type airflows using a multiphase approach. *Indoor Air*. 2006;16:296–312.

55. Chen C, Zhao B. Some questions on dispersion of human exhaled droplets in ventilation room: answers from numerical investigation. *Indoor Air*. 2010;20:95–111.

56. Gao N, Niu J, Morawska L. Distribution of respiratory droplets in enclosed environments under different air distribution methods. *Build Simul*. 2008;1:326–335.

57. Fisk WJ, Faulkner D, Sullivan D, Bauman F. Air change effectiveness and pollutant removal efficiency during adverse mixing conditions. *Indoor Air*. 1997;7:55–63.

58. Krajčík M, Simone A, Olesen BW. Air distribution and ventilation effectiveness in an occupied room heated by warm air. *Energy and Buildings*. 2012;55:94–101.

59. Rim D, Novoselac A. Ventilation effectiveness as an indicator of occupant exposure to particles from indoor sources. *Building and Environment*. 2010;45:1214–1224.

60. Sandberg M. What is ventilation efficiency? *Building and Environment*. 1981;16:123–135.

61. Olmedo I, Nielsen PV, Ruiz de Adana M, Jensen RL, Grzelecki P. Distribution of exhaled contaminants and personal exposure in a room using three different air distribution strategies: Distribution of exhaled contaminants. *Indoor Air*. 2012;22:64–76.

62. Yang J, Sekhar C, Cheong DKW, Raphael B. A time-based analysis of the personalized exhaust system for airborne infection control in healthcare settings. *Science and Technology for the Built Environment*. 2015;21:172–178.

63. Ai Z, Hashimoto K, Melikov AK. Airborne transmission between room occupants during short-term events: Measurement and evaluation. *Indoor Air*. May 2019:ina.12557.

64. Gao NP, Niu JL, Perino M, Heiselberg P. The airborne transmission of infection between flats in high-rise residential buildings: Particle simulation. *Building and Environment*. 2009;44:402–410.

65. Li X, Niu J, Gao N. Spatial distribution of human respiratory droplet residuals and exposure risk for the co-occupant under different ventilation methods. *HVAC&R Research*. 2011;17:432–445.

66. Bivolarova M, Ondráček J, Melikov A, Ždímal V. A comparison between tracer gas and aerosol particles distribution indoors: The impact of ventilation rate, interaction of airflows, and presence of objects. *Indoor Air*. 2017;27:1201–1212.

67. Tang M, Zhu N, Kinney K, Novoselac A. Transport of indoor aerosols to hidden interior spaces. *Aerosol Science and Technology*. 2020;54:94–110.

68. Ai Z, Mak CM, Gao N, Niu J. Tracer gas is a suitable surrogate of exhaled droplet nuclei for studying airborne transmission in the built environment. *Build Simul*. 2020;13:489–496.

69. Li X, Niu J, Gao N. Co-occupant's exposure to exhaled pollutants with two types of personalized ventilation strategies under mixing and displacement ventilation systems. *Indoor Air*. 2013;23:162–171.

70. Gupta JK, Lin C-H, Chen Q. Characterizing exhaled airflow from breathing and talking. *Indoor Air*. 2010;20:31–39.

71. Persily AK, de Jonge L. Carbon dioxide generation rates for building occupants. *Indoor Air*. 2017;27:868–879.

72. Yang L, Wang X, Li M, et al. Carbon dioxide generation rates of different age and gender under various activity levels. *Building and Environment*. September 2020:107317.

73. Nazaroff WW, Alvarez-Cohen L. *Environmental Engineering Science*. New Delhi: Wiley-India; 2011.

74. Sandberg M, Sjöberg M. The use of moments for assessing air quality in ventilated rooms. *Building and Environment*. 1983;18:181–197.

Measured Influence of Overhead HVAC on Exposure to Airborne Contaminants from Simulated Speaking in a Meeting and a Classroom

Brett C. Singer[1]*, Haoran Zhao[1], Chelsea V. Preble[1,2], William W. Delp[1], Jovan Pantelic[1,3], Michael D. Sohn[1], Thomas W. Kirchstetter[1,2]

[1]Indoor Environment Group, Energy Analysis and Environmental Impacts Division, Building Technologies and Urban Systems Division, Energy Technologies Area, Lawrence Berkeley National Laboratory, Berkeley, CA, USA

[2]Department of Civil & Environmental Engineering, University of California, Berkeley, CA, USA

[3]Center for the Built Environment, University of California, Berkeley, CA, USA

List of Figures

Window Coverings

Figure S1. Foam panels on exterior of windows during Conference experiments.

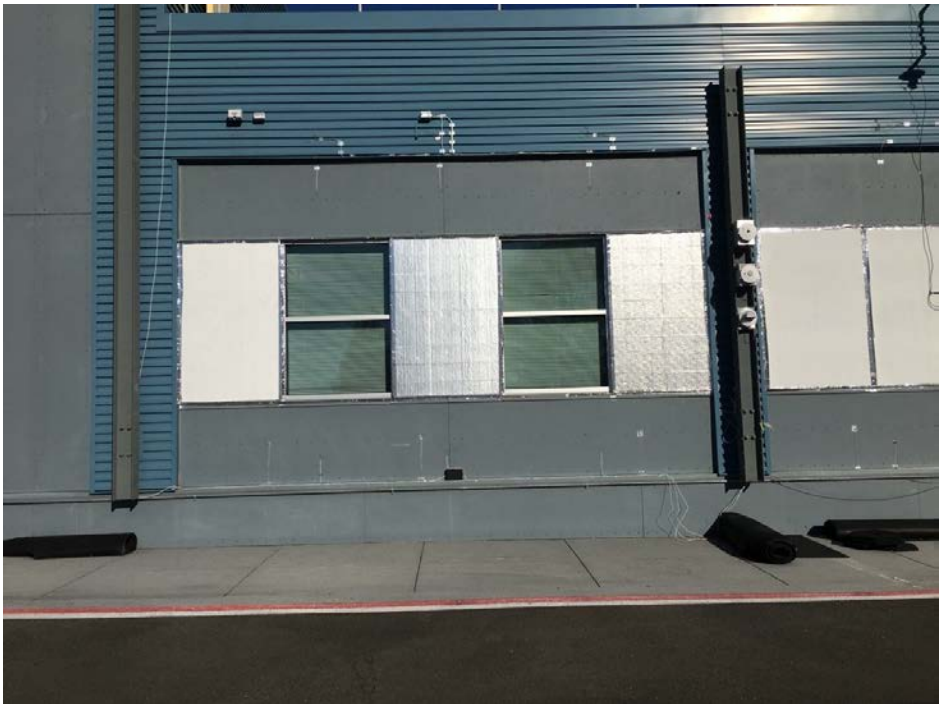

Figure S2. Exterior of cell with foam panels removed from two of five window sections during Classroom experiments.

Figure S3. Windows with foam panels removed during Classroom experiments.

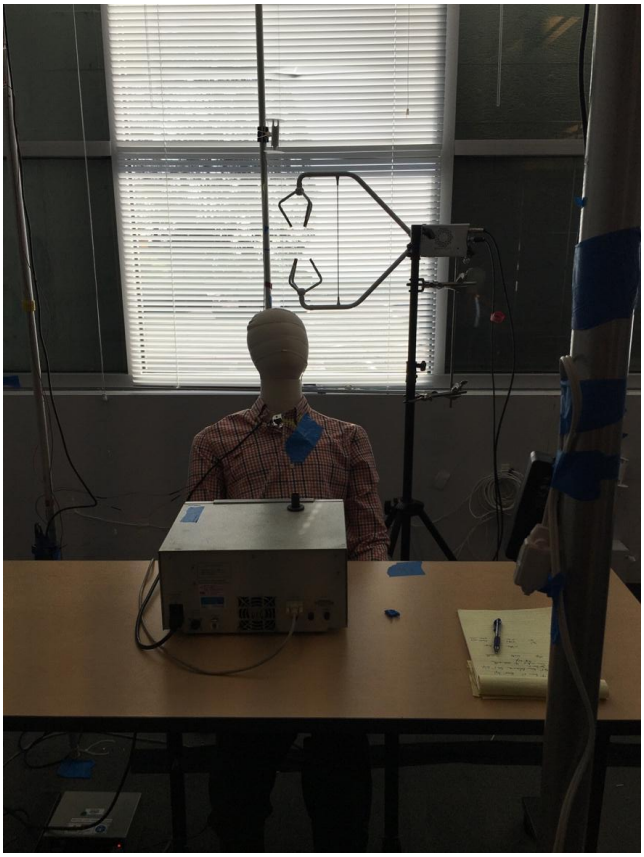

Figure S4. Positioning of blinds during Classroom experiments.

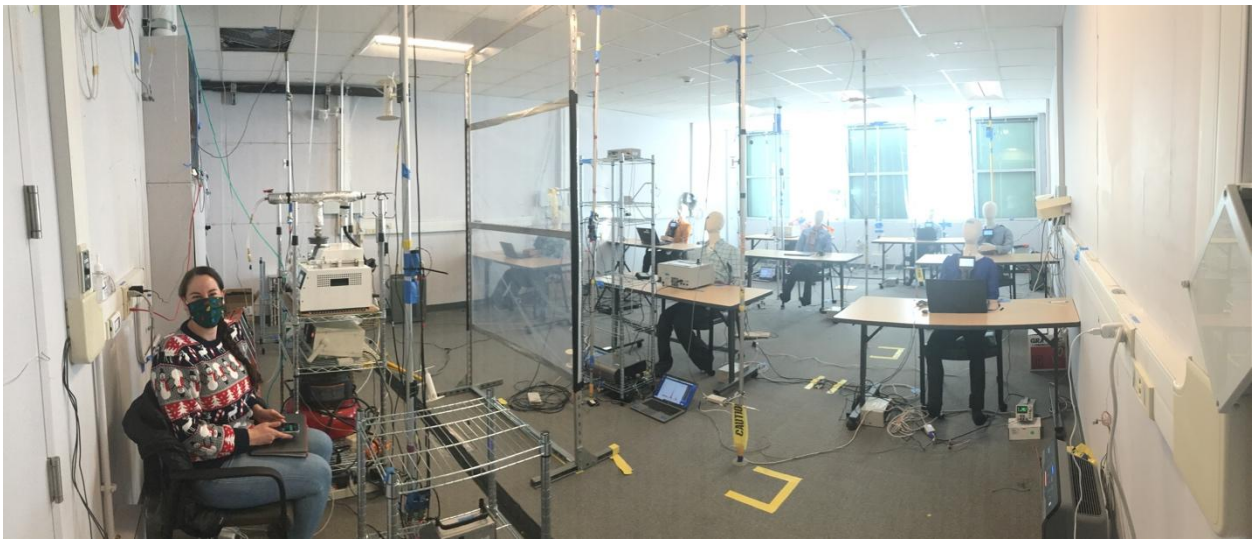

Figure S5. Classroom configuration with release at Teacher position and free-standing barrier placed between Teacher and R1C positions.

Figure S6. Conference room configuration.

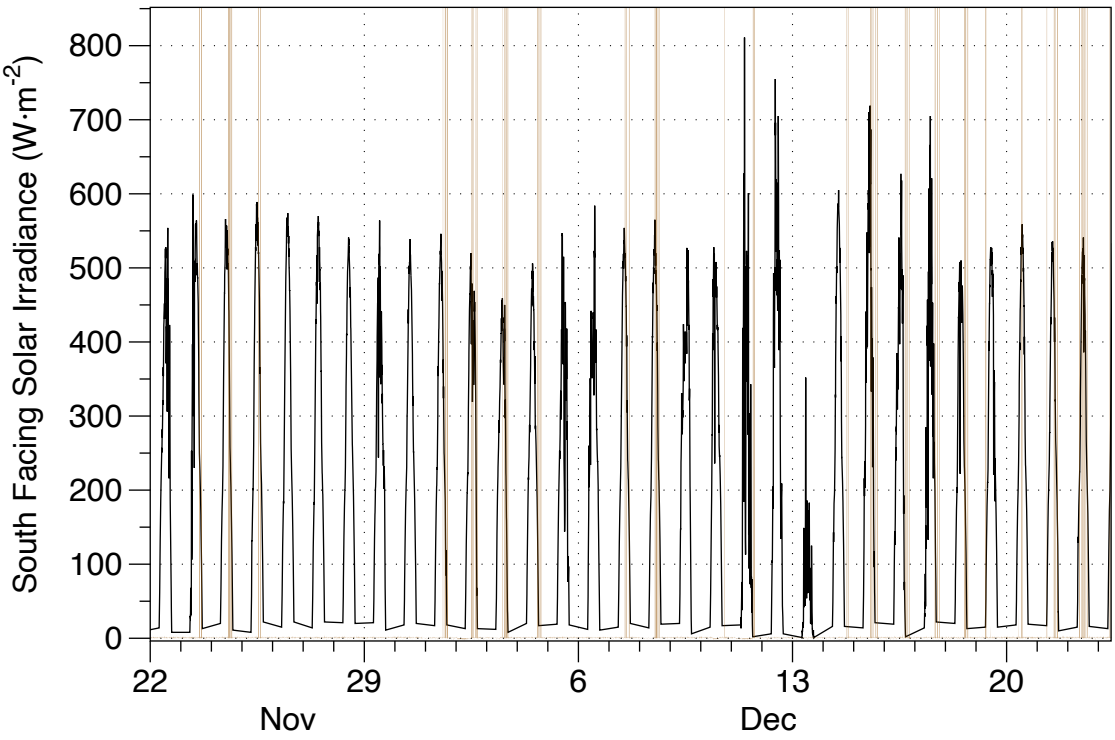

Figure S7. Direct solar irradiance on Southern Wall of FLEXLAB during period of experiments.

Other Heat Sources

For most of the experiments, seven laptops were deployed on the desks in front of the manikins. Four of the laptops were used to drive and log data from the hot sphere anemometers and another three sonic anemometers that were deployed during experiments but are not reported in this paper. The power used by each laptop ranged from 8–30 W and the average total power during logging over one day of experiments was 93 W. The power consumption of the particle counter, CO_2 meter, raspberry Pi and anemometer ranged from less than 2 W to 22 W, resulting in a total of ~160 W during the experiment. During some experiments with PACs running, each PAC added a power consumption of ~50 W when operated on high speed.

During 11 experiments conducted Dec 4–10, heating devices used on the tracer release apparatus released consumed and thus released an average of ~16W. During 28 experiments from Dec 14 to 23, a Flow Focusing Monodisperse Aerosol Generator (FMAG, TSI Model 1520) was deployed in the room to release a mixture of CO_2, air, and particles. The average power consumption of the FMAG and heat tape wrapped around the outlet was 44 W during experiments.

Tracer Release Assemblies

The first assembly (A, Figures S8–9) was a brass manifold designed to join a flow of pure CO_2 with the output of a Collison nebulizer that introduced 2 μm diameter polystyrene latex spheres (PSL) into 5.7 LPM of air then out through a nozzle of 0.95 cm internal diameter (0.71 cm^2 area). An optical particle counter (OPC) pulled 2.83 LPM from a tee just before the outlet to quantify particles at the release. For experiments reported in this paper, the OPC was placed on the shoulder of the manikin at the release location with its outlet oriented in the same direction as

the main release tube (Figure S9). This setup was used in two experiments with the nebulizer and OPC as described and two with the nebulizer and OPC removed.

Figure S8. Assembly A configured with Collison nebulizer to release 2 µm PSL particles.

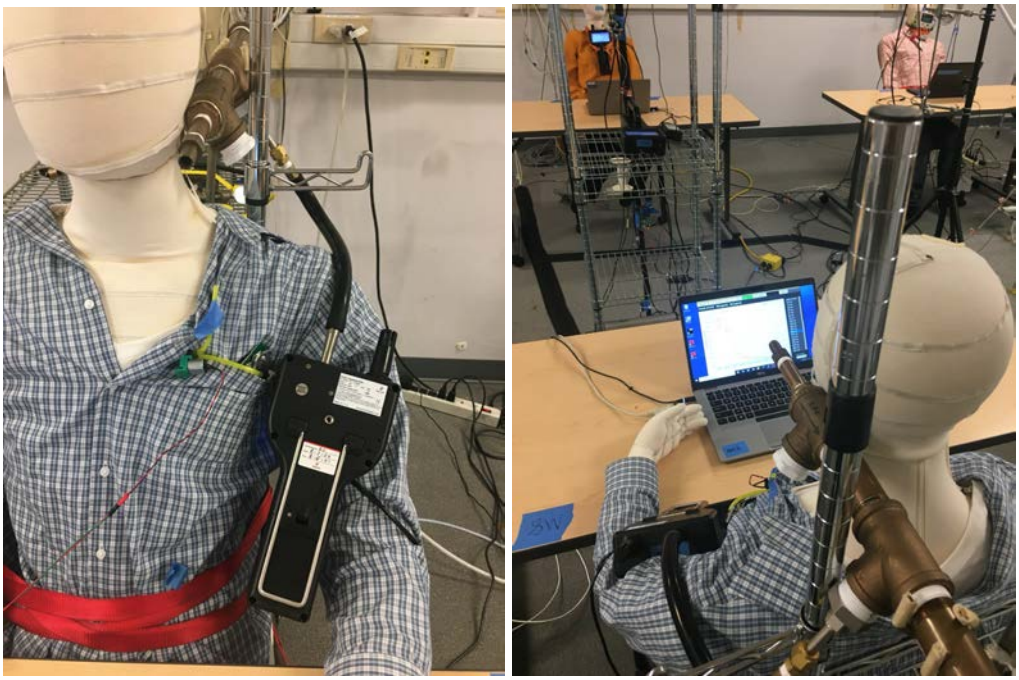

Figure S9. Assembly A with outlet of OPC pointing in the same direction as release nozzle.

Assembly B was a 30 cm section of 1.11 cm internal diameter (0.97 cm^2 area) flexible hose attached to a section of aluminum strut for support (Figure S10). In five experiments, flows of 10 LPM air and 2.55 LPM CO_2 were combined in a wye feeding the release at room temperature. The assembly was modified to enable a heated release by wrapping the aluminum and hose section with an off-the-shelf heating pad with four thermostatically controlled settings followed by a blanket (Figure S11). A second heating pad was wrapped around a section of inline flexible copper tubing to preheat the mixed stream of air and CO_2; 11 experiments were conducted with this setup.

Figure S10. Unheated Assembly B on manikins at East and North seated positions.

Figure S11. Assembly B with heating pads on supply and at release.

Assembly C was a brass manifold that connected the output of the FMAG that was used to release 8–10 μm particles into 10 LPM of air with a flow of 5.1 LPM CO_2. The manifold was heated (in most experiments to a setpoint of 37 ºC) and insulated. The outlet was a brass pipe with 1.5 cm internal diameter (1.8 cm^2 area). This was used in 17 experiments in the conference room and 11 in the classroom. The flow through the FMAG was 10 LPM air.

CO_2 Cross-Calibration Process

The K30s were cross-calibrated to a single research grade instrument on a daily basis. The research grade instrument was a PP Systems SBA-5 CO_2 analyzer. A 5-point calibration (from 493 to 2466 ppm) was performed on the SBA-5 after the experiments using diluted standard CO_2 gas. This calibrated SBA-5 was visually checked at the low end to the closest reporting sensors on the BEACO_2N network (http://beacon.berkeley.edu/about/). The overnight lows and periods where the room was well ventilated agreed with the expected outdoor values. For the daily cross-calibrations we visually identified periods where the room was expected to be well mixed and selected 2 to 5 windows, each ranging from 5 to 10 min, covering a range of values from background to highest well mixed for the day. The same time window was used for all intervals each day, ensuring equal weighting. The concentrations measured by each K30 during those windows were fit to the calibrated SBA-5 readings linearly via a python StatsModels ordinary least squares (OLS)2 routine to develop the slope and intercept for each device on each day. Then, the sensor consistency was checked by calculating relative standard deviation across all of the days (6 to 22) for the slopes. By dropping the lowest and highest 2 values, the relative standard deviations ranged from 0.09 to 3.3% with a median value of 1.5% (IQR 1.3–1.8%), indicating that the calibrations were very stable across the days. For the three days where we did not have valid intervals for performing cross-calibrations, we used the median values of the daily cross calibrations for each of the sensors.

CO_2 Baseline Concentration Projection

Baseline concentrations ($C_{b,i}$) were projected from just before the release to the end of the post-release period. This baseline was spatially and temporally dynamic, depending on the airflow conditions for the room and whether the chamber returned to the starting condition of outdoor CO_2 levels between experiments.

For experiments with no AHU operation, the outdoor air exchange was considered to be zero, resulting in no loss of CO_2 from the cell. Post-release periods with no AHU operation had concentration profiles consistent with this assumption on no CO_2 loss. There was evidence of a small amount of air leakage in some experiments, in which experiments with AHU operation but no intentional outdoor air exchange sometimes appeared to have a non-zero decay as concentrations decreased after the cell was well-mixed. This is thought to result from air being pulled into the AHU through leaks in the outdoor air damper with the same quantity of air being exhausted through leaks in the exhaust air damper. The outdoor air exchange rates estimated for these experiments varied from 0 to 0.18 h^{-1}. Given the uncertainties in these estimates and the minor impact that such small AERs would have over a 30–45-minute period of analysis, we assumed no outdoor air exchange when projecting the baseline for these experiments.

For experiments with no intentional outdoor air exchange, no researcher present, and evidence of good mixing throughout the cell prior to the release, the concentration just before the release was assumed as a constant baseline through the experiment. If the cell was not well mixed before the release—e.g., if the observed concentrations in the room indicated that the most recent emission event mixed primarily in the room and not fully throughout the plenum—it was assumed that the room air concentration would have decreased by first order decay to the level representing a perfectly mixed cell. For example, in experiment 1125B, the concentrations measured just before release at all location were higher than the expected well-mixed concentration of 1192 ppm; the baseline of each location was thus projected as first order decay from the initial, elevated concentration measured at each location towards 1192 ppm. The decay would not actually be first order as air coming into the room from the plenum would have a steadily increasing concentration with the plenum. However, since differences between the observed, imperfectly-mixed concentrations pre-release and the concentrations expected with perfect mixing in the cell were small, the errors of treating this as a first order decay are small. For the experiments without intentional ventilation and with a researcher present and seated to operate the aerosol generation device, a CO_2 generation rate of 0.23 LPM was assumed (L. Yang et al. 2020). The baseline was then taken as the expected uniform, well-mixed concentrations in the cell just before release ($C_{0,i}$) following a steady release from the researcher, as indicated in Equation S1. E_R represents CO_2 release from the researcher inside ($m^3\ h^{-1}$) and V is the cell volume (237 m^3).

$$C_{b,i}(t) = C_{0,i} + \frac{E_R}{V}t \tag{S1}$$

For experiments with intentional ventilation, the room and plenum were determined to be mixed at the time of each release. Thus, concentrations in the room (and cell) would have decayed toward the background, outdoor level at the air exchange rate (λ, h^{-1}) indicated by the outdoor airflow and cell volume. This well-mixed baseline in the cell was projected for each experiment using a mass-balance equation that accounts for constant sources and removal processes, as described in Appendix D of Nazaroff and Alvarez-Cohen (2011):

$$C_{b,i}(t) = C_{0,i}\ exp\ (-\lambda t)\ + \left(\frac{E_R}{\lambda V} + C_{out}\right)[(1 - exp\ (-\lambda t)] \tag{S2}$$

In this equation, units of mL m^{-3} or ppm are used for CO_2.

Theoretical Well-Mixed Exposure Calculation

To calculate theoretical concentrations, we assumed the released CO_2 was instantaneously well mixed in the volume of the cell. For experiments without intentional ventilation, the decay due to air change rate was assume to be zero. During an experiment with recorded release time from t_0 to t_r and decay time that extended from t_r to t_d, the CO_2 concentration in the room during the release period was calculated as:

$$C_T(t) = C_0 + \frac{E_T + E_R}{V}t \quad if\ t_0 < t \leq t_r \tag{S3}$$

where $C_T(t)$ is the well-mixed CO_2 concentration at time t, E_T is the CO_2 release rate, and C_0 is theoretical well-mixed concentration at the start of the release which is assumed to be the outdoor concentration. The concentration during the decay period is given by:

$$C_T(t) = C_0 + \frac{E_T + E_R}{V} t_r + \frac{E_R}{V}(t - t_r) \quad if\ t_r < t \leq t_d \tag{S4}$$

The theoretical well-mixed baseline concentration ($C_{b,T}$) during both the release and decay periods only considered the emission from the researcher if present, and is the same as Equation S1.

The time-integrated incremental theoretical concentration over both release and decay period is:

$$\begin{aligned} X_T &= \int_{t_0}^{t_d} \left(C_T - C_{b,T}\right) dt \\ &= \int_{t_0}^{t_r} C_0 + \frac{E_T + E_R}{V} t\ dt + \int_{t_r}^{t_d} C_0 + \frac{E_T + E_R}{V} t_r + \frac{E_R}{V}(t - t_r) dt \\ &- \int_{t_0}^{t_d} C_0 + \frac{E_R}{V} t\ dt \\ &= -\frac{1}{2}\frac{E_R}{V} t_d^2 - \frac{1}{2}\frac{E_R + E_T}{V} t_r^2 + \frac{1}{2}\frac{E_R}{V}(t_d - t_r)^2 + \frac{E_R + E_T}{V} t_r t_d \end{aligned} \tag{S5}$$

This results in a final formula that is not related to C_0, such that that theoretical increments were only related to the emission rates and duration of the experiment.

For experiments with intentional ventilation, the ventilation rates (λ) were firstly calculated using the measured outdoor air flow rates over the room volume. Assuming well-mixed conditions, the CO_2 concentration in the room during the release period was calculated as:

$$C_T(t) = C_0 exp\ (-\lambda t)\ + \left(C_{out} + \frac{E_R + E_T}{\lambda V}\right)(1 - exp(-\lambda t)\ ) \quad if\ t_0 < t \leq t_r \tag{S6}$$

As such, the time-integrated concentration during release is given by:

$$\int_{t_0}^{t_r} C_T\ dt = \left(C_{out} + \frac{E_R + E_T}{\lambda V}\right) t_r + \frac{1}{\lambda}(C_0 - C_{out} - \frac{E_R + E_T}{\lambda V})[(1 - exp\ (-\lambda t_r)] \tag{S7}$$

Similarly, concentration and time integrations during the decay period were determined with:

$$\begin{aligned} C_T(t) &= C_{T,t=tr} exp\ [-\lambda(t - t_r)] \\ &+ \left(C_{out} + \frac{E_R}{\lambda V}\right)[1 - \exp\ (-\lambda(t - t_r)] \quad if\ t_r < t \leq t_d \end{aligned} \tag{S8}$$

$$\int_{t_r}^{t_d} C_T dt = \left(C_{out} + \frac{E_R}{\lambda V}\right)(t_d - t_r) + \frac{1}{\lambda}(C_{T,t=tr} - C_{out} - \frac{E_R}{\lambda V})[1 - exp\ (-\lambda t_d)] \tag{S9}$$

With ventilation, the baseline will also decay across the release and decay experimental periods. Here, the CO_2 emitted by researcher, if present, is the same as given in Equation S2, and the integrated baseline during both release and decay is:

$$\int_{t_0}^{t_d} C_{b,T} dt = \left(C_{out} + \frac{E_R}{\lambda V}\right)(t_d) + \frac{1}{\lambda}(C_0 - C_{out} - \frac{E_R}{\lambda V})[1 - exp\ (-\lambda(t_d)] \tag{S10}$$

Thus, the time-integrated incremental theoretical concentration over both the release and decay periods is:

$$X_T = \int_{t_0}^{t_d} \left(C_T - C_{b,T}\right) dt = \int_{t_0}^{t_r} C_T \, dt + \int_{t_r}^{t_d} C_T dt - \int_{t_0}^{t_d} C_{b,T} dt \quad \text{(S11)}$$

As with Equation S5, this results in a final formula that is independent of C_0 and instead only related to the emission rates and duration of the experiment.

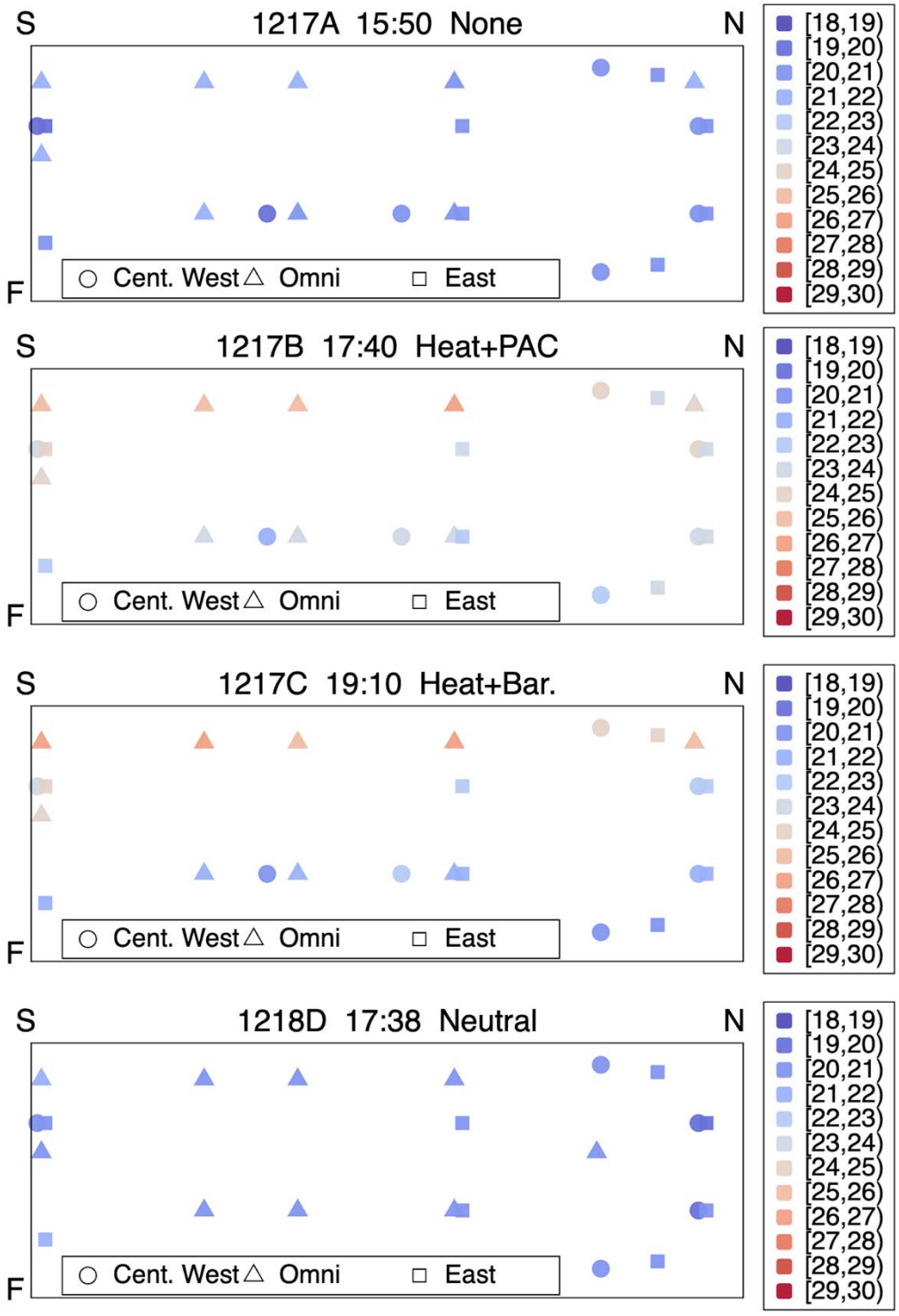

Figure S12. Vertical temperature profiles along the south (S) to north (N) transect in the meeting room with all windows covered. F indicates the floor. Squares and circles show thermistors in eastern third and center-west two thirds of the room, as indicated in Figure 1. Triangles show omnidirectional anemometers. Experiment 1217B had one portable air cleaner on high speed and 1217C had a barrier in front of an elevated manikin at the North position. Note the stratification and slightly warmer temperatures at the south (covered) window when heating.

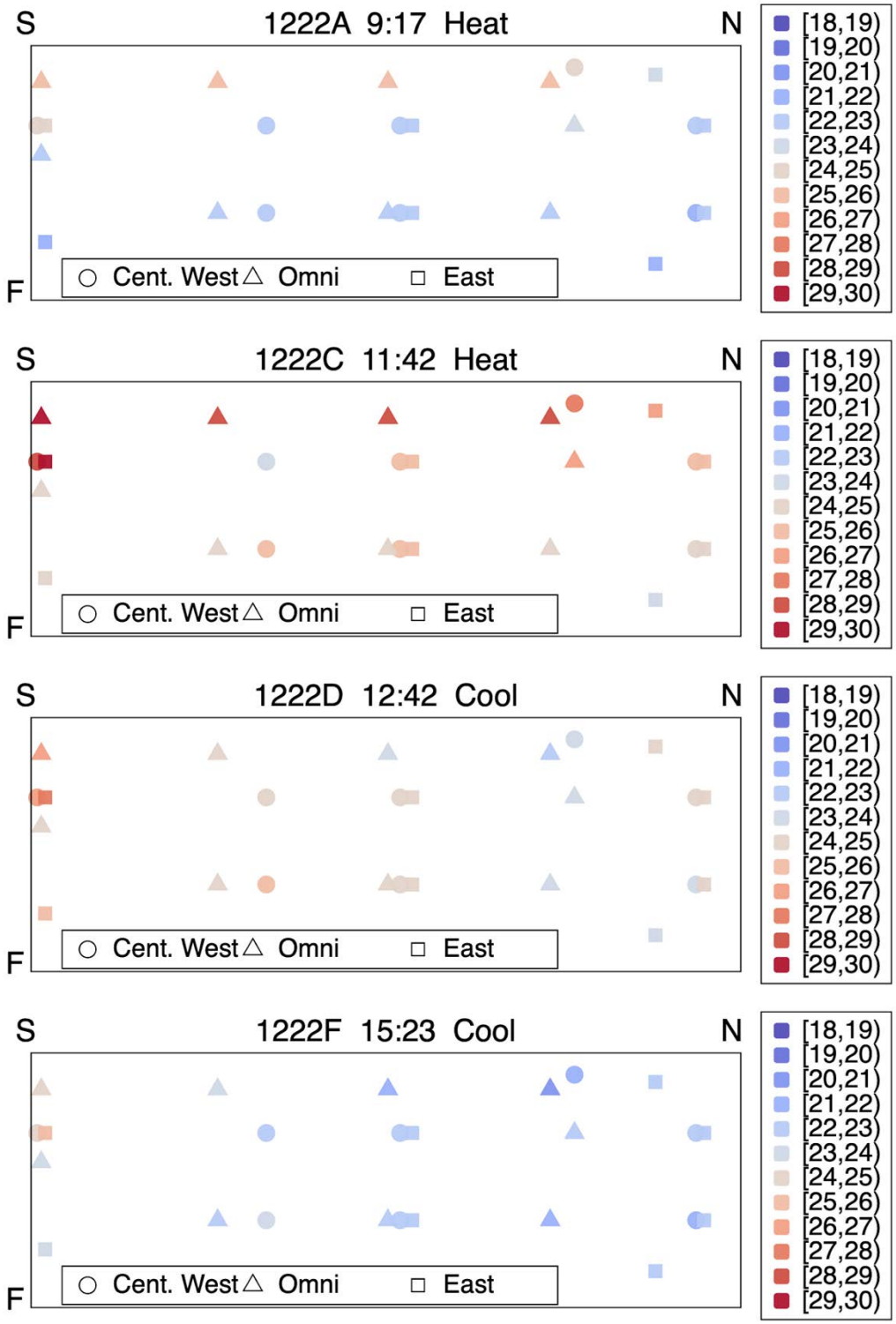

Figure S13. Vertical temperature profiles from South to North (left to right) in the classroom with two windows. Refer to prior caption for symbol notes. Experiment 1222B was heating and 1222E was cooling. Note similar patterns for the two heating and two cooling experiments despite different ranges of temperatures.

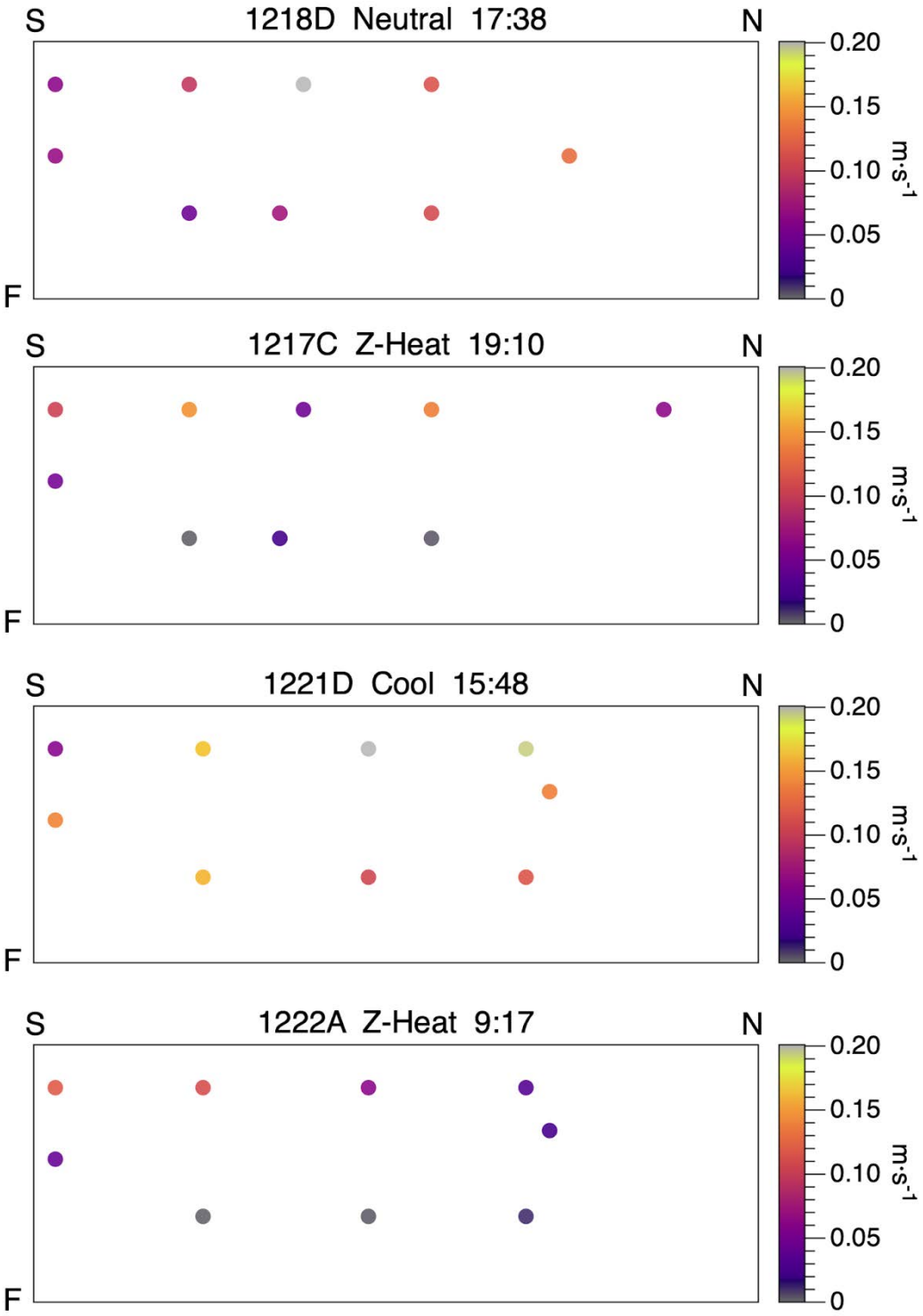

Figure S14. Air speed data from selected experiments in meeting (top two panels) and classroom (bottom two panels). Details of experiments provided in Table 1. Data from anemometers at locations shown in Figure 1 except Northern sensor in 1217C, which was just to the West of North-most manikin.